ADDIS ABABA UNIVERSITY

ADDIS ABABA INSTITUTE OF TECHNOLOGY

AFRICAN RAILWAY CENTER OF EXCELLENCE

Optimal Method of Generating Power at the Train Rooftop for the Auxiliary Power Supply System

Case Study: Solar and Wind Power Generation on Electric Multiple Units (EMU) at Addis Ababa Light Rail Transit System (AALRT)

A Thesis in Railway Engineering (Rolling Stock)

By

Osbert Matsiko

July, 2019

A Thesis

Submitted in Partial Fulfillment of the Requirements for the Degree of Master of Science in Railway Engineering (Rolling Stock)

APPROVAL

The undersigned have examined the thesis entitled '**Optimal method of generating power at the train rooftop for the auxiliary power supply system**' presented by **Osbert Matsiko**, a candidate for the degree **of Master of Science in Railway Engineering (Rolling Stock)** and hereby certify that it is worthy of acceptance.

Dr. Celestin Nkundineza		
Advisor	Signature	Date
Abdulkadir Aman Hassen (PhD)		
Internal Examiner	Signature	Date
Yilma Tadesse Birhane (PhD)		
External Examiner	Signature	Date
Chair person	Signature	Date

UNDERTAKING

I certify that research work titled “Optimal method of generating power at the train rooftop for the auxiliary power supply system” is my own work. The work has not been presented elsewhere for assessment. Where material has been used from other sources it has been properly acknowledged / referred.

…..……

Osbert Matsiko

ABSTRACT

This research aims at exploring the optimal method of generating energy on the rooftop of the train when it's in motion, for the case of Addis Ababa Light Rail Transit system (AALRT).The sources of energy considered are solar and wind energy. The collected energy can be used to power the auxiliary services like air conditioning, door opening and closing, LED display and others.

To be able to achieve this, the solar and wind resource assessment was done for Addis Ababa to assess the viability of this project. It was found out that Addis Ababa receives 4kWh/m^2/day to 7kWh/m^2/day annually. The ambient wind speeds are rather low for wind energy harvesting and i.e less than 2 m/s. From the literature reviewed, the induced wind speeds are almost half the vehicle speed which is about 4m/s. This is still low and therefore a ducted turbine was recommended. This would increase the wind speed to 15m/s which is sufficient for energy generation.

It was found out that 21 solar panels would be installed that would be able to generate 24.6kWh/m^2/day and using a ducted turbine would increase wind power generated from 73.3W to 3.8kW.

The solar and wind system components were sized and representative components i.e. components with similar specifications were selected from HOMER (Hybrid Optimization Model for Multiple Energy Resources) and cost optimization and sensitivity analysis were done. Optimization results obtained indicated solar would be more cost effective than wind with Cost of Energy as 0.0947. To simulate the actual conditions on ground, the system was connected to the grid and it was still realized that using solar would be more cost effective than using wind or grid connection. In fact, when the system is connected to the grid, the cost of energy increases to 0.251. This further confirmed that using solar energy is still the most optimal method.

In the end, it was recommended that for wind energy, the project would be more viable if implemented on the Ethio-Djiboute line which has relatively higher vehicle speeds and few vehicle stopovers as compared to AALRT. However, solar energy can be implemented at AALRT since it's able to supply for sufficient power at minimal cost.

ACKNOWLEDGMENTS

I dedicate this thesis to my dear wife and daughter. Without you, this wouldn't have been possible. You kept me going even I felt like giving up.

I also would like to thank my Supervisor, Dr. Celestin Nkundineza, your timely support and guidance was very helpful in this thesis. I can't take this for granted and may God reward you abundantly.

And finally, special thanks to World Bank and ARCE for giving me this chance to study in a place away from home which has become home. It's been a worthwhile experience and I look forward to applying the knowledge I acquired here for the growth and development of my country.

TABLE OF CONTENTS

LIST OF TABLES

LIST OF FIGURES

CHAPTER 1 INTRODUCTION

1.1 Background

Energy demand in developing countries is increasing at a fast rate. A case in point is Ethiopia whose energy need is increasing mainly due to high population estimated at 105 million and the resultant economic activity [1]. As a result, the government of Ethiopia has decided to increase the installed generation capacity to 2GW by constructing the Grand Ethiopian Renaissance dam with installed capacity of 6000MW and solar farms at Metahala [2]. Also, Ethiopia has set up two wind energy projects namely Ashegoda Wind Park (near Mekele) of 120MW and the other is Adama Wind Park producing 153MW [3]. Therefore, to meet the increased energy demand, it's clear the government is exploring all possible alternatives to generate power to meet this demand.

Ethiopia receives 4.55 to 6.5 kWh/m^2/day annual average of solar irradiation throughout the country [4]. The current installed solar capacity is 5MW and most of this energy is used by off grid telecom systems which account for 87% of the total installations. Other applications include domestic use, water pumping and health systems [5]. On the other hand, Ethiopia has exploitable reserve of 100 GW wind energy with an average speed of 3.5 – 5.5 m/s flowing for 6 hours per day, the total wind power so far generated is approximately 171MW [6] which has been increased to 324MW currently [7].

It's clear therefore that energy saving is very crucial if Ethiopia is to meet the ever increasing energy demand. This can be achieved by using innovative ways to harness any energy from all the available sources and avoiding wastage. A case in point is the Addis Ababa Light Rail Transit System (AALRT) that relies purely on hydro power grid connection for motive power and other auxiliary services like door operation and air conditioning yet if solar panels and wind turbines were installed on the rail vehicles. Then, some energy would be generated to provide power to cater for these services. This would save some energy which could be supplied to other needy areas and would also reduce the cost of electricity to Ethiopian Railways Corporation (ERC). Thus, this project aims at harnessing this untapped energy to support auxiliary services by using two different means.

Previous studies have been done on this; *Gupta* [8] obtained the patent of the design of wind and solar powered railway coaching stock. In his invention, the system comprises of solar panels mounted on the roof of the vehicle and the wind turbines are attached under the coach berries. The wind induced by the train motion is captured and used to run the turbines and the electricity generated is used to run the air conditioning load. The solar panels generate substantial power during the day to meet the basic requirement of illumination and cabin load [8]. *Jeffery* [9] suggests installing solar panels on the roof and side walls of the train stations and buildings along the train route and also on the roof of the train. *Gajanur* [10] did a similar project about installing solar panels on the roof of the train to power cameras installed on the face of the train to monitor up to 2km of the track as a way of minimizing train accidents in India. Also Indian Railways on July 14, launched the first solar-powered DEMU (diesel electrical multiple unit) train from the Safdarjung railway station in Delhi. A total of 16 solar panels, each producing 300 WP, are fitted in six coaches. The solar panels generate about 17 units of power in a day which enables the lighting system in the coach [11].

From the literature reviewed, the researchers focused on generation of solar and wind energy from moving trains however no optimization was done to determine the most cost effective method. Therefore, using AALRT as a case study, this research aimed at getting an optimal method for generating solar and wind energy on the train rooftop for the auxiliary systems.

If this research is implemented, then then daily cost of electricity incurred by ERC should reduce since this energy is free and only needs an initial capital investment. Secondly, the energy saving on the hydro electricity grid can be used for other purposes or can be supplied to another needy area.

1.2 Problem statement

To be able to satisfy the ever increasing power demand arising from the ever increasing population, the Ethiopian government should not only invest in increasing the generation capacity but should encourage innovative ways of generating and saving the already generated power [2]. Secondly, for quicker return on investment (ROI) in the railway industry, the daily operating costs have to be minimized as much as possible.

One of the ways to achieve the above goals is by reducing the power consumption by using other conventional sources that require just an initial capital investment and minimal

operational costs. The saved power can be supplied to other areas in need thus increasing the electricity coverage in due course. At AALRT, other sources of energy like wind and solar can be used to power the auxiliary service or if generated in sufficient amounts, can provide the necessary motive power which would help save some energy and reduce the daily operation costs.

Therefore, this project aims at determining the optimal method of generating power required by the auxiliary systems from the roof of the train.

1.3 Objectives

1.3.1 Main Objective

The main objective of this project is to determine an optimal method of generating energy i.e. solar and wind energy required for the auxiliary systems by installing solar panels or wind turbine on the roof of the train.

1.3.2 Specific objectives

- To study the solar and wind energy potential of Addis Ababa
- To determine the total auxiliary power requirement for the multiple units at AALRT
- To determine the available train rooftop area and the number of solar panels that can be installed
- To size the solar and wind system components and obtain their specifications and prices in order to carry out a cost optimization.
- To carry out a PV/wind hybrid cost optimization using HOMER software and compare results against the existing grid connection.

1.4 Delimitation

Due to limited time and financial resources, this research stopped at the sizing of wind and solar system components and carrying out a cost optimization for the same systems. To be able to be implemented, further studies may have to be carried out and more funding should be availed.

CHAPTER 2 LITERATURE REVIEW

2.1 Introduction

Energy sources can be categorized in two forms namely; conventional (non-renewable) and non-conventional (renewable) energy sources. Renewable energy is energy generated from sources at the same rate as it is being utilized for example; wind, hydro, solar PV, biomass, solar thermal and geothermal whereas non-renewable energy is consumed without being replaced i.e. it gets depleted after sometime and is not normally environmental friendly. Fossil fuels like coal, oil and natural gas are examples of non-renewable energy sources [12].

Renewable energy systems are environmental friendly because they don't emit any dangerous gasses into the atmosphere. Air pollution affects public health, agriculture and ecosystems. In addition, the consumption of this energy doesn't result in depletion of resources. This is the reason why it is referred to as "green" or "clean" energy [12].

2.2 Solar Energy

The sun is the largest energy source of life and is the ultimate source of most renewable energy on earth. The total amount of energy, which is irradiated from the sun to the earth's surface, equals approximately 10,000 times the annual global energy consumption. Solar energy can be used to generate electricity directly by using photovoltaic (PV) modules and by using solar thermal systems [13]. This study only focused on photovoltaic modules.

The light of the sun, which reaches the surface of the earth, consists mainly of two components: direct sunlight and indirect or diffuse sunlight, which is the light that has been scattered by dust and water particles in the atmosphere. Photovoltaic cells not only use the direct component of the light, but also produce electricity when the sky is cloudy [13].

2.2.1 Photovoltaic Systems (PV)

Photovoltaic (PV) is a method of generating electrical power by converting solar radiation into direct current electricity using semiconductors that exhibit the photovoltaic effect. PV power generation uses solar panels comprising a number of cells containing a semi-

conducting material.

As long as light is shining on the solar cell, it generates electrical power. When the light stops, the electricity stops.

The solar cells that are used on calculators and satellites are photovoltaic cells or modules. This PV module consists of many PV cells wired in parallel in order to increase current and in series to produce a higher voltage. A PV panel consists of a number of PV modules and an array consists of any number of PV panels. Individual PV cells are typically only a few inches in diameter, but multiple cells can be connected to one another in modules, modules can be connected in arrays, and arrays can be connected in very large systems [14]. PV panels convert sunlight to DC power. The PV generated electricity is "silent", low in maintenance and does not need fuel or oil supplies. However, PV energy is available when enough irradiance is accessible [14]. Figure 2-1 details these definitions.

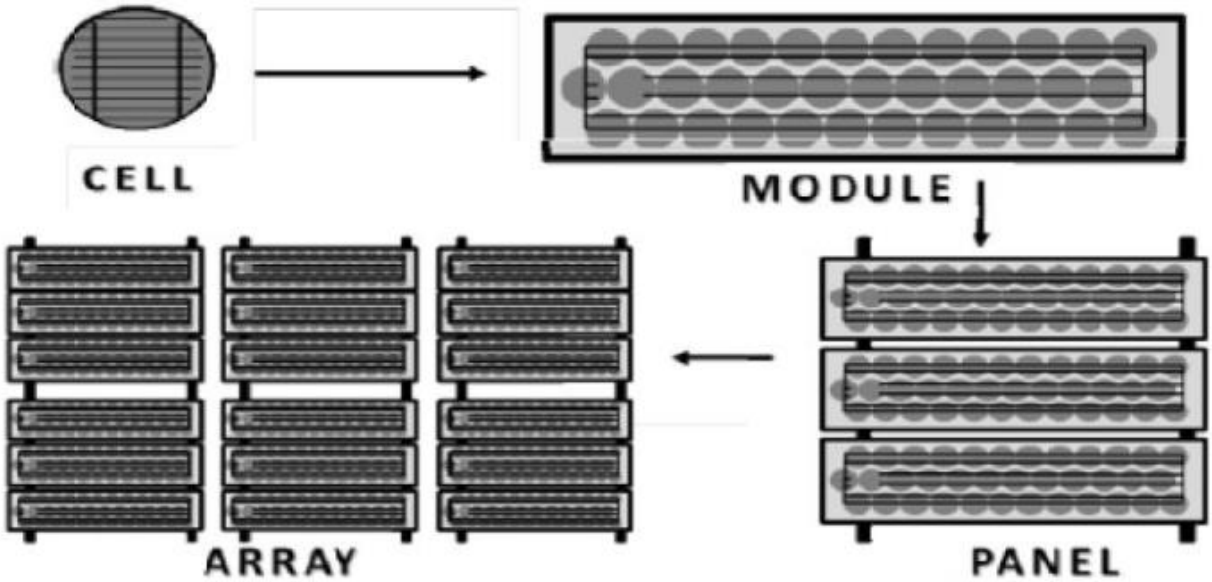

Figure 2-1: PV Diagram [12]

2.2.2 Working Principle of PV Cells

PV cells convert sunlight directly into electricity by taking advantage of the photoelectric effect. Cells are constructed from semiconductor materials coated with light-absorbing materials. When photons in sunlight strike the top layer of a PV cell, they provide sufficient energy to knock electrons through the semiconductor to the bottom layer, causing a separation of electric charges on the top and bottom of the solar cell. Connecting the bottom layer to the top with a conductor completes an electrical circuit and allows the

electrons to flow back to the top, creating an electric current and enabling the cycle to repeat with more sunlight [2].

2.2.3 PV Module and Array

The basic building block of a PV system is a solar cell however it can't be used individually since it is not able to supply enough voltage and current to any electronic device. Therefore, many PV cells are connected in parallel or in series in order to achieve as high voltage and current as possible. Cells connected in series increase voltage output while cells connected in parallel increase current.

A typical photovoltaic system is made of 36 individual 100cm^2 silicon photovoltaic cells and auxiliary devices which are lead-acid batteries with a typical voltage of 12 V. This system has the capacity of producing more than 13V during cloudy days and can charge a 12 V battery [2].

2.2.4 Factors Affecting PV system performance

i. Irradiance

The fact is that irradiance varies throughout the day [15]. The angle of the sun, passing clouds, hazy weather, and air pollution can affect irradiance levels. However, the total energy received by the system from the sun remains relatively constant from year to year. Typically, energy from the sun only varies between 5-10% of the average in a given year. Consequently, quality solar energy output projections can be made based on the past years [15].

ii. Shading

Shading may be caused by any obstructions in the vicinity of PV arrays that interfere with the solar window, especially obstructions to the east, south and west of an array [16]. This includes trees, towers, power lines, buildings and other structures, as well as obstructions close to and immediately around the array, such as antennas, chimneys, plumbing vents, dormer windows and event from other parts of the array itself. Shading of PV arrays can also be caused by accumulated soiling on the array surface, which can be particularly severe in more arid regions requiring regular cleaning to ensure maximum system output. For large PV systems with multiple parallel rows one in front of another in the array, one row of modules can shade the one in back if the rows are too closely spaced [16].

iii. Soiling

Dirty solar panels produce less electricity [17]. Soiling refers to dust, dirt, and other debris settling on the surface of the solar panels. This blocks sunlight from reaching the solar cells and reduces solar system performance [17]. In areas with frequent rain, soiling is not usually significant. Rapid soiling can also occur on systems located near construction sites and other places that produce dust. Cleaning the system may be undertaken regularly to keep the modules clean.

iv. Array Orientation

The orientation and tilt of a system impacts how much of the available irradiance the system can collect [18]. PV arrays should be oriented toward the solar window to receive the maximum amount of solar radiation available at a site, at any time. The closer an array surface faces the sun throughout every day and over a year without being shaded, the more energy that system will produce, and the more cost-effective the PV system becomes with respect to alternative power options [19]. Similar to sun position, the orientation of PV arrays is defined by two angles called the azimuth and tilt angles.

v. Array Azimuth Angle

Azimuth angle is the direction an array surface faces based on a compass heading or relative to due south [20]. North is 0^o or 360^o, east is 90^o, south is 180^o and west is 270^o. Unless side shading or local weather patterns dictate otherwise, the optimal azimuth angle for facing tilted PV arrays is due south (180^o compass heading) in the northern hemisphere, and due north in the southern hemisphere [20].

vi. Array Tilt Angle

Array tilt angle is the angle between the array surface and the horizontal plane. Generally, the higher the site latitude, the higher the optimal tilt angle to maximize solar energy gain [20]. A horizontal array has a zero degree tilt angle, and a vertical array has a 90^o tilt angle. The array azimuth angle has no significance for horizontal arrays, because they are always oriented horizontally no matter how they are rotated [20].

2.2.5 Solar radiation Estimation

The light from the sun which reaches the surface of the earth consists of mainly direct and indirect sunlight also known as diffuse sunlight, which is the light that has been scattered by dust and water particles in the atmosphere. PV cells use both components whether the sun is shining or not [21].

To determine the solar generation potential of a site, it is important to assess the average total solar radiation received over the year. Unfortunately, most times this data is not available, the only information available is always sunshine duration data [21]. Given the knowledge of the number of sunshine hours and local atmospheric conditions, this data can be used to estimate monthly average solar radiation with the help of empirical formulas [22]. These equations are explained as follows;

$$\boldsymbol{H = \bar{H}_0\left(a + b\left(\frac{\bar{n}}{N}\right)\right)} \quad 2.1$$

Where;

H is the monthly average daily radiation on a horizontal surface (MJ/m^2)
$\bar{H}_0$ is the monthly average daily extraterrestrial radiation on a horizontal surface (MJ/m^2)
$\bar{n}$ is the monthly average daily number of hours of bright sunshine
N is the monthly average of the maximum possible daily hours of bright sunshine
a and b are regression coefficients of solar radiation, known as extraterrestrial radiation $\bar{H}_0$ on a horizontal plane outside the atmosphere, is given by equation 2.2

$$\bar{H}_0 = \frac{24*3600*G_{sc}}{\pi}\left(1 + 0.033 * cos\left(\frac{360n_d}{365}\right)\right) * \left(cos\phi cos\delta sin\omega_s + \frac{\pi\omega_s}{180} sin\emptyset sin\delta\right) \quad 2.2$$

Where;

n_d is the day number, G_{sc} is the solar constant (1367 W/m^2), $\emptyset$ is the latitude of the location (°), δ is the declination angle (°), which is the angular position of the sun at solar noon, with respect to the plane of the equator and its value in degrees is given;

$$\delta = 23.45\sin\left(248 + n_d\left[\frac{360}{365}\right]\right) \quad 2.3$$

The solar hour angle (ωs) is the angular displacement of the sun east or west of the local meridian; morning negative, afternoon positive. The solar hour angle is equal to zero at

solar noon and varies by 15 degrees per hour from solar noon. The sunset hour angle s w is the solar hour angle corresponding to the time when the sun sets and it is given by;

$$\omega_s = \cos^{-1}(-tan\emptyset tan\delta) \quad 2.4$$

The maximum possible sunshine duration N is given by;

$$N=\frac{2}{15}\omega_s \quad 2.5$$

n_d is t the day of the year which is a continuous function of time. It can be conventionally obtained from table 2-1 shown below.

Table 2-1: Recommended average days for months and values of n by months [23]

Month	n for i^{th} day of the month	For the average day of the month		
		date	n, day of year	δ declination
January	i	17	17	-20.9
February	31+i	16	47	-13.0
March	59+i	16	75	-2.4
April	90+i	15	105	9.4
May	120+i	15	135	18.8
June	151+i	11	162	23.1
July	181+i	17	198	21.2
August	212+i	16	228	13.15
September	243+i	15	258	2.2
October	273+i	15	288	-9.6
November	304+i	14	318	-18.9
December	334+i	10	344	-23.0

The regression constants a and b for M number of data points can be calculated from the following equations.

$$a = \frac{\Sigma\frac{\bar{H}}{\bar{H}_0}\Sigma\left((\frac{\bar{n}}{\bar{N}})^2\right)-\Sigma\frac{\bar{n}}{\bar{N}}\Sigma\frac{\bar{n}}{\bar{N}}\frac{\bar{H}}{\bar{H}_0}}{M\Sigma(\frac{\bar{n}}{\bar{N}})^2-\Sigma(\frac{\bar{n}}{\bar{N}})^2} \quad 2.6$$

$$b = \frac{M\Sigma\frac{\bar{n}}{\bar{N}}\frac{\bar{H}}{\bar{H}_0}-\Sigma\frac{\bar{n}}{\bar{N}}\Sigma\frac{\bar{H}}{\bar{H}_0}}{M\Sigma(\frac{\bar{n}}{\bar{N}})^2-\Sigma(\frac{\bar{n}}{\bar{N}})^2} \quad 2.7$$

Results estimated in this way are compared with the data which is obtained from sources such as NASA's surface solar energy data set or the SWERA global meteorological

database. Drake and Mulugetta developed sets of constants a and b for various locations in Ethiopian [24]. In this thesis, regression coefficients developed in their work were used.

2.3 Wind Energy

2.3.1 Introduction

Wind is another potential source of renewable energy. Wind is the movement of air caused by pressure differences within the atmosphere. This pressure differences exert a force that causes air masses to move from a region of high pressure to one of low pressure. That movement of air is referred as wind. Such pressure differences are caused primarily by uneven heating effects of the sun on the Earth's surface. Thus, wind energy is form of solar energy [25].

Wind power is the transformation of wind energy into more utilizable forms, typically electricity using wind turbines. The wind turbine captures the wind's kinetic energy of air mass by a rotor consisting of two or more blades [13]. Figure 2-2 shows a typical wind turbine system.

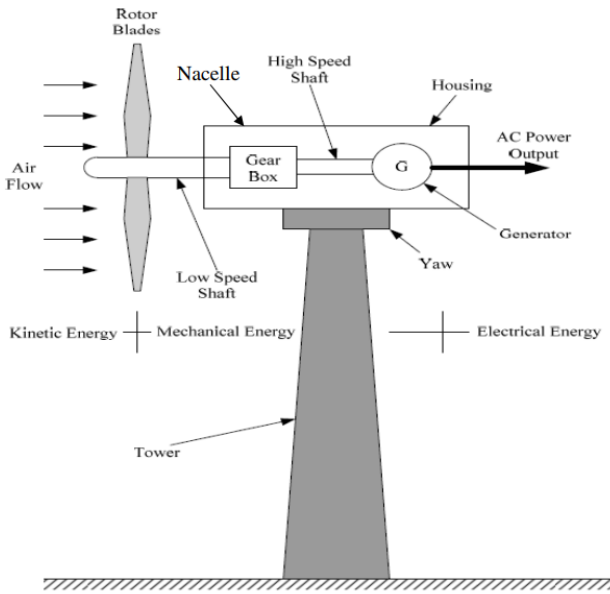

Figure 2-2: Block Diagram of a Wind Energy Conversion System [22]

2.3.2 Wind Turbines

Wind turbines convert kinetic energy of the wind into mechanical energy. If the mechanical energy is directly used by the machinery, then it's termed as a windmill but if

mechanical energy is converted into electricity, then the machine is called a wind generator. Different designs of wind turbines have evolved overtime but most of them comprise a rotor that turns round blades propelled by lift or drag forces which results in its interaction with the wind. Depending on the position of the rotor axis, wind turbines are classified into vertical axis and horizontal axis [26].

The horizontal axis turbine, HAWT is the most common type of turbine and are of different types; the upwind which faces the wind (tower behind rotor) and the downwind arrangement (tower in front). Another type is the vertical axis, VAWT that uses drag and lift as the driving forces [27].These are shown in figure 2-3.

One of the advantages of the upwind turbines is that the tower does not act as an obstacle for the wind hitting the rotor however the flow behind the passing blade is affected by the tower and causes a slight drop in power. When the blade passes the tower, it also decreases the drag on the construction which can cause an on / off bending process causing fatigue however this is normally taken into account when designing the turbine. Also, the upwind design needs a control system that helps the nacelle turn straight into the wind [27].

In downwind turbines, the tower shades a rotor blade each time it passes and causes power losses compared to the upwind design. The advantage with these turbines is that the nacelle is self-adjusting and doesn't require any control system however the main disadvantage is that there is always a problem of twisting of the cable inside when the nacelle turns in the same direction repeatedly [27].

The VAWT´s are not as commercial and economically competitive as the HAWT´s. Some of the VAWT types suffer from low efficiency due to design difficulties as well as the problem with operation close to the ground. Parts of the vertical turbines will therefore receive low speed winds causing power losses. To keep the construction upright, it also needs to be supported with guy cables attached to the ground. The vertical turbine is not in need of yaw control, which ofcourse is an advantage and the wind always hits the turbine tangentially [27].

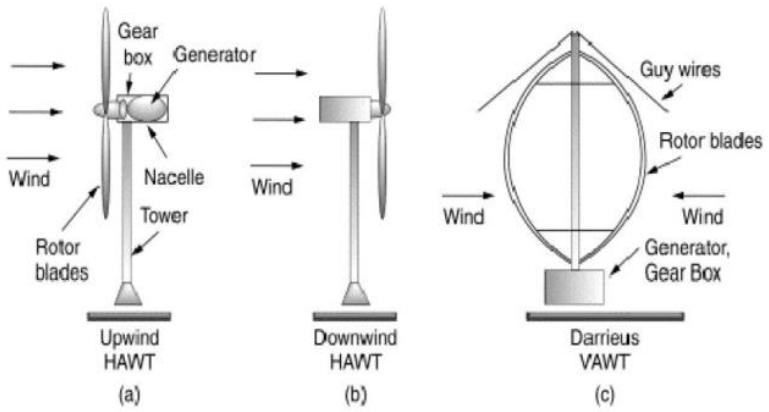

Figure 2-3: Horizontal Axis wind Turbines (HAWT) and Vertical Axis Wind Turbines (VAWT) [27].

The different parts are described below [2];

Generator

The generator is connected to the high speed shaft and is the component of the system that converts the rotational energy of the shaft into an electrical output.

Tower

The tower is used to support the nacelle and rotor blades and typically made of rolled, tubular steel, and built and shipped in sections because of its size and weight. Common tubular towers incorporate a ladder within the hollow structure to provide maintenance access. Small-scale towers range in height from 24-35m and its weight depends on the material from where it is manufactured.

Nacelle

The rotor attaches to the nacelle, which sits atop the tower and includes the gear box, low- and high-speed shafts, generator, controller, and brake. A cover protects the components inside the nacelle. Some nacelles are large enough for a technician to stand inside while working rotor in emergencies.

Controller

The controller starts up the turbine at wind speeds of about 3.5 to 7.2m/s and shuts off the machine at about 30m/s depending on the rated speed of the turbine and this also depends on the type of turbine.

High-speed shaft: Drives the generator.

Low-speed shaft: The rotor turns the low-speed shaft at about 30 to 60 RPM depending on the turbine type.

Pitch: Blades are turned, or pitched, out of the wind to keep the rotor from turning in winds that are too high or too low to produce electricity.

Rotor: The blades and the hub together are called the rotor.

Yaw drive: Upwind turbines face into the wind; the yaw drive is used to keep the rotor facing into the wind as the wind direction changes. Downwind turbines don't require a yaw drive; the wind blows the rotor downwind.

Yaw motor: Powers the yaw drive.

Electronic equipment: Such as controls, electrical cables, ground support equipment and interconnection equipment.

2.3.2 Working Principle of Wind Turbines

The blade, using aerodynamic lift, captures energy from wind in order to turn the shaft. In small wind turbines the shaft usually drives the generator directly. The generator converts the mechanical energy into electricity. The shaft power causes coils to spin past alternate poles of magnets allowing electric current to flow. If a permanent magnet device is being used, the opposite occur: current flows as magnets spin past coil windings. Most small wind turbines use a permanent magnet alternator. Large wind turbines usually use either induction generator or a synchronous generator. In addition, in large wind turbines the shaft connected to the generator via a gearbox those steps up the rotational speed for the generator [2].

2.3.3 Wind Energy extraction

The kinetic energy of the wind is extracted by using the appropriate wind turbine which converts it into mechanical rotation energy at the shaft. The rotational energy is converted into electrical energy through the transmission system. The transmission system consists of the rotor shaft with bearings, brake(s), an optional gearbox, as well as a generator and optional clutches. The energy extracted from the wind can be computed by equation 2.8.

$$P_w = \frac{1}{2} \rho A V^3 \qquad 2.8$$

Where:

$\rho = Density\ of\ air\ (kg/m^3$

A= the swept area (m^2)

P_w= Power in the wind (W)

V= Instantaneous Wind Velocity

Energy conversion from free-flowing fluid streams is limited because full energy extraction implies decrease of fluid velocity (decrease of kinetic energy of the stream), down to zero which is impossible. Some fluid may not pass through the turbine and may simply flow around it (bypass it). This limitation is expressed in terms of Betz limit defined by the power coefficient Cp which can be computed from equation 2.9.

$$C_p = \frac{Rotor\ power}{Power\ in\ the\ wind} \qquad 2.9$$

The power coefficient, CP, is a function of the axial induction factor. The optimum of this function (which is a maximum value for CP) is 0.5926 (=16/27) [28, 26, 13]. Thus the electrical power output from the wind turbine can be expressed by equation 2.10.

$$P_w\,out = 0.5 * \rho_t C_p\, \rho\, Av^3 \qquad 2.10$$

Where, P_w out = output power of wind turbine

$\rho_t = Overall\ efficiency\ of\ the\ transmission\ system$

C_p = Power coefficient

The power coefficient and efficiency of wind turbines vary greatly from manufactures to manufacturers. As a result, the power output of wind turbines vary from turbine to turbine and is given by power curve which plots the output power of a turbine against wind speed.

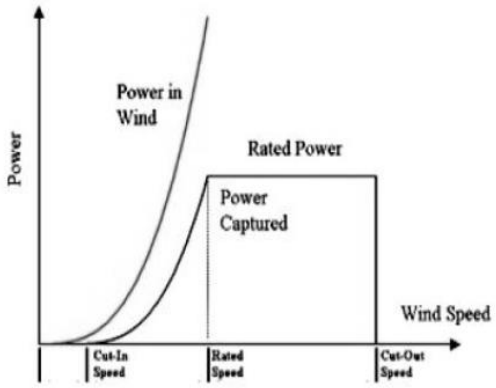

Figure 2-4: Power Curve of a Wind Turbine [25]

The wind speed at which the turbine starts generating electrical power is called the cut-in speed. The rated wind speed is the wind speed at which the turbine operates at its maximum efficiency of energy conversion. Rated power is the power output at the wind speed which is equal to or above the rated wind speed. The cutout speed is the wind speed at which the turbine may be shut down to protect the rotor and drive train machinery from damage or high wind stalling characteristics [28].

2.3.4 Wind Speed Measurement

The wind speed is measured by an instrument called anemometer. There are several types but the most common is the cup anemometer which has three or four cups attached to a rotating shaft. When the wind hits the anemometer, the cups and shaft rotate. The angular speed of the spinning shaft is calibrated in terms of the linear speed of the wind. Normally, the anemometer is fitted with a wind vane to detect the wind direction. A data logger collects wind speed and wind direction data from the anemometer and wind vane respectively.

While measuring the wind speed, it's important to set the measuring equipment high enough to avoid turbulence created by trees, buildings or other obstructions. Readings become more useful when taken at the height where the wind turbine is to be installed.

If the measurement of the wind speed isn't made at the turbine hub height, then the measured wind speed can be adjusted to the hub height using either the logarithmic law which assumes that the wind speed is proportional to the logarithm of the height above ground or the power law which assumes that the wind speed varies exponentially with height.

Using logarithmic law, the wind speed at a certain height can be given by equation 2.11 [13].

$$v(z).ln\left(\frac{z_r}{z_0}\right) = v(z_r).ln\left(\frac{z}{z_0}\right) \quad 2.11$$

Where,

Z_r is reference height (m)

Z- height where wind speed is determined (m)

Z_0 – Measure of surface roughness (0.1 to 0.25 for crop land)

v(z) wind speed at height Z_m (m/s)

v (Z_r) wind speed at the reference height (m/s)

Using power law, the wind speed at a certain height above ground level can be given as follows [16]:

$$v_2 = v_1\left(\frac{h_2}{h_1}\right)^{\alpha} \quad 2.12$$

Where:

v_1 is wind speed measured at the reference height h_1 (m/s)

v_2 is wind speed estimated at height h_2 (m/s)

α is ground surface friction coefficient. The different friction coefficients are shown in table 2-2

Table 2-2: Friction Coefficient α of Various Terrains [13].

Terrain type	Friction Coefficient, α
Lake, ocean and smooth, hard ground	0.10
Foot-high grass on ground level	0.15
Tall crops, hedges and shrubs	0.20
Wooded country with many trees	0.25
Small town with some trees and shrubs	0.30
City area with tall buildings	0.40

2.4 Solar and Wind Energy in Railway

The train is a hub of energy that can be harvested to supply power to the grid or to various auxiliary systems on it. When the train is in motion, it creates an air pressure in the opposite

direction; it compresses the air in the front of it and pushes it to its sides, thereby creating a vacuum at its rear and sides as it moves forward. To fill up this vacuum, the mass air flow rushes into the sides and the rear of the train as it moves forward. The kinetic energy created by this wind flow can therefore be used to generate electricity [29].

Another method is to integrate solar modules into traditional roof materials of the train to generate clean energy or by installing solar modules on the rooftop. This method promotes effective use of roof space [29].

Different research has been conducted regarding the utilization of wind and solar energy on trucks, buses and trains and the influence of external factors on the component performance. Use of wind and solar energy in moving trains is quite and innovative approach [30].

There are two major types of wind turbine: horizontal axis wind turbine (HAWT) and vertical axis wind turbine (VAWT), each one defines the axis of the blades rotation with respect to ground. For this application, it's advisable to use VAWT because of the following reasons:

- Beneficial at high wind speed typical for moving train
- Robust structure as HAWT will produce significantly produce more air drag
- HAWT's blades are more likely to undergo mechanical damage due to higher thrust
- Blades of the HAWT must be adjusted to wind direction by using pitch system which is not required for VAWT
- Starting torque for VAWT is higher compared to HAWT
- For VAWT, components such as gear box and generators are combined into compact structure [29].

For solar systems, they convert light energy directly into electricity using semiconductor technology in the form of solar/PV cells. The power output of a PV system is determined by the type and area of the PV material and the incident solar radiation. Mathematically, it can be expressed by equation 2.13 below [22] [31].

$$P_{pv} = A_C \eta_{mp} \eta e \, G_T \qquad 2.13$$

P_{pv} = power output of PV array

A_c=the array area

η_{mp} =the maximum power point efficiency of the array (≈14%)

η_e =the efficiency of power conditioning equipment (≈90%)

G_T=the incident solar radiation on the array

Previous research on railway green energy systems have come up with wind systems installed on rooftop, trackside and even between the rails. Others have developed solar systems installed on the rooftop of the train or canopy at the train stations. Some have also combined both systems however no optimal method has been determined by any of these researchers. This chapter summarizes the previous studies that have been done.

2.4.1 Combined Wind and Solar Energy Systems

Gupta [8], invented a system of harnessing green energy from the moving railway coaching stock. The solar energy and train motion induced wind energy is tapped to meet energy requirements of the railway coaching stock. The invention can be used in Electric Multiple Units (EMU), Diesel Multiple Units (DMU), Subway, Tram and Metro Railways.

The major objective of this invention was to generate solar and wind energy with solar panels mounted on the roof of the train and the wind turbines mounted under the coach belly to reduce the drag that would otherwise be created if the wind turbines were installed on the roof top. Another objective of this invention was to do away with DC-AC conversion by designing independent circuits for AC and DC loads. The DC loads are powered directly by the solar system and the AC loads are powered by the AC generator run by the wind turbine. This minimizes the power losses as a result of this conversion.

The invention uses openable flaps at the end face of the coaches. The flaps open by air thrust generated by train motion exceeding a certain value. The wind is guided through ducts installed between existing wall linings of the coaches and under the belly of the coaches. The air is then ejected through nozzles to the turbines forming high velocity jets. With this invention, it was estimated that 419.6kW was generated by a combination of both systems [8].

2.4.2 Wind Energy harvested from train rooftop

Garvit et al**,** [32]**,** developed a wind energy system that employs the concept of vertical axis wind turbine and radial hydraulic turbine. When the fluid enters the spiral casing, with some velocity it first passes through the guide vanes and then thorough the runner blades. The fluid spins the shaft on the runner which is connected to the dynamo. The air then disperses from the crevices between the runner and the blades. The essence of the radial turbine concept is when air enters the spiral casing, it initially gives a drive to each blade and then finally hits one of the blades with significant impact and during this episode the wind speed is constant. The proposed system is shown in figure 2-5 [32].

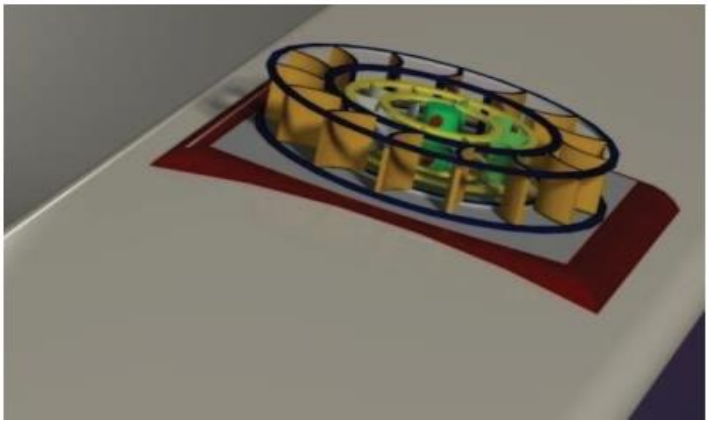

Figure 2-5: Proposed Wind Turbine [32].

Figure 2-5, shows the system in detail. It has two sets of blades, the inner ones are mobile and are responsible for the rotation of the shaft whereas the outer blades are for the guiding wanes which facilitate the shaft to rotate in one direction irrespective of the direction of the train [32].

Using wind speeds as obtained by *Habib Nasser, 2013* [33], the calculations indicated that about 3600W was generated by this system.

Srinivasm et al [34] installed a wind turbine on the roof of the rail coach but an air duct was added to reduce the drag force and also to avoid the wind turbine from hitting the overhead structures. The duct is designed in such a way that it reduces the drag force and increases the velocity of the air that hits the turbine blades.

As shown in figure 2-6, the duct is designed like a converging nozzle at the entry side, so the velocity of the air that hits the turbine is increased whereas it's designed as a diverging

nozzle on the exit side so that the air gets expanded and cooled before it gets into the atmosphere without any resistance that would affect the performance of the train [34].

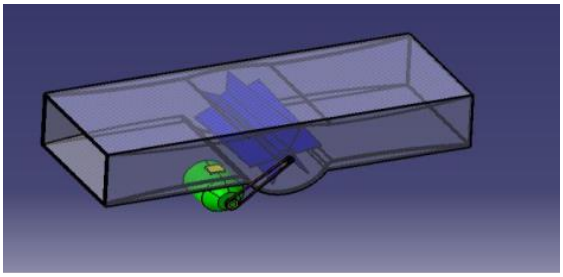

Figure 2-6: Proposed duct and Wind turbine System [34]

In Addition to having a duct as shown above, Sindhuja.B, [29] proposes having an auxiliary system that sucks the air or it is positioned in such manner that the opposing wind flow is naturally forced into the duct, the air is then compressed with a set of impellers and is stored in an agitation tank. When the speed of the train or the major input speed is below the desired level, then a governor sets the boosting system to inject high pressure air through a gun nozzle over the turbine to maintain the speed of the turbine rotation. This system can generate a huge amount of power [29].

The high pressure air is injected at variable speeds as the turbine input by using a gun like mechanism to maintain the desired speed even during slow motion of the train. This ensures a steady, high speed, fluctuation less high torque input to the generator to produce large scale power output [29].This system is able to produce five times more power than any other conventional system.

In [30] and as shown in figure 2-7, the researchers decided to install a series of wind turbines on the train rooftop because; there are higher wind speeds and less obstacles at the roof than in the sides and there is also sufficient space to accommodate all the system components. The proposed systems comprises a HAWT and an air duct which concentrates and guides the air flow directly to the blade of the turbine. The duct also creates a shelter for the system from precipitation and other mechanical damage.

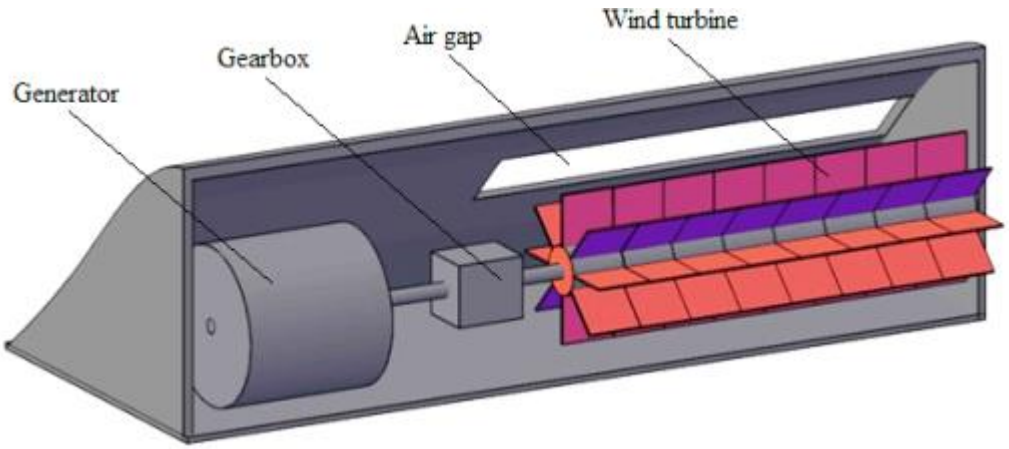

Figure 2-7: Wind Power System. The horizontal gaps are equal in length as the turbine and work as a duct [30]

With 10 such systems installed on the train rooftop, the system would generate 126.7kW, this amount of power is sufficient to overcome the air drag and supply sufficient power to the load [30].

2.4.3 Wind energy harvested along the railway track

Avinash et al. [35] harvested wind energy by installing wind turbines across the railway tracks. The gust of wind generated by the running trains can be used to rotate the wind turbines and thus power can be generated. In the wind turbine design, by adjusting the turbine height and considering different wind speeds, the system was able to generate 200W to 600W which is sufficient to light the track.

Saleh et al. [36] invented a rail mounted wind turbine that has a pivotable housing and is placed between rails of a rail track. The housing can move at least into one upward position or downward position and includes a wind turbine. The wind turbine has a blade that moves when a force such as wind force is applied to provide mechanical energy to generate electrical power. A controller controls the movement of the pivotable housing into at least one upward position and at least one downward position. This invention is shown in the figure 8 below.

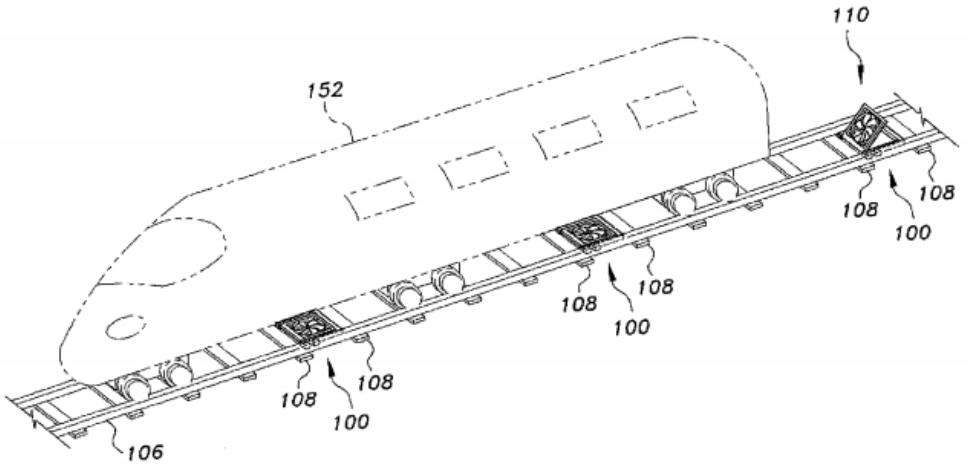

Figure 2-8: Wind Turbine installed between the rails [36]

2.4.4 Solar System Installed along the track

David et al [37] made an invention that provides a method by which rail systems can use air space above tracks and right of way for generating traction power for electric powered rail vehicles as shown in figure 2-9. Through the design and installation of rail-specific solar photovoltaic canopy modules, replicated and joined together in assemblies of various lengths, transit districts, rail agencies and operators can generate energy for rail vehicle traction power supply.

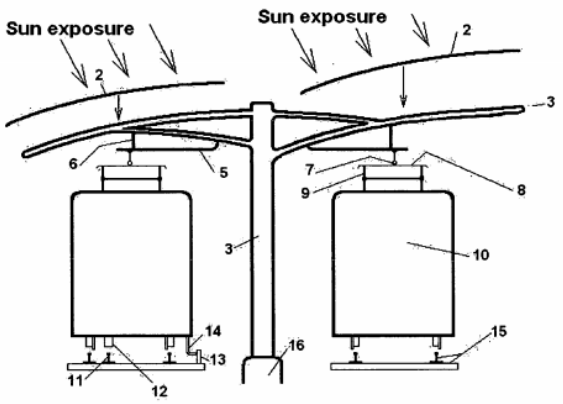

Figure 2-9: Proposed Canopy [37]

Syed et al. [9] propose having solar train stations along the route to generate power. The generated power can then be fed into the grid or the overhead line to be used by the locomotive. Since railway transport is restricted to predetermined track ways that are normally isolated, the possibility of scratch and dents is minimal as compared with road transport. This also make it possible to install solar panels on structures such as platforms, track sides and passenger shades.

A typical solar power station should be designed to receive maximum solar radiation throughout the day, it should be free from any obstructions like buildings. A typical solar station is shown in figure 2-10.

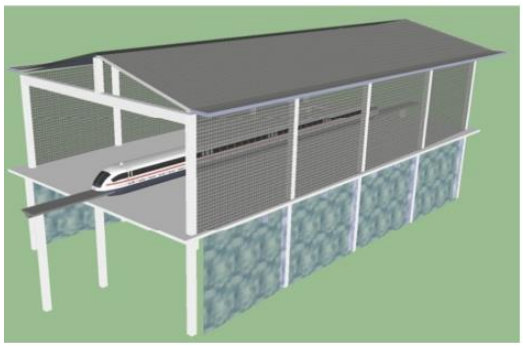

Figure 2-10: Solar Train Station as proposed [9]

2.4.5 Solar system installed on the Train

Shravanth et al**.** [38] conducted a study to determine the fuel savings that would be realized if solar panels were installed on the rooftop of the trains in India. It was found out that one rail coach would be able to produce 18kWh electricity in a day which would translate to an annual fuel saving of 1700litres. Since Indian railways operates a large fleet of trains, this would further translate to 105.5 million liters of fuel per year [38]. Therefore, massive energy savings can be realized if this solar system is used.

Nanditha [10] designed a railway track monitoring system. The system would include a solar panel installed on the roof of the train, a camera installed in front of the train to monitor at least 2 km of the track. The camera would be powered by this solar system. This would enable the train crew to monitor up to 2km of the track in real time and act accordingly [10].Therefore, in some instances, simple solar systems can be designed to supply power to different systems.

Prasanth [39] the researchers here try to explain innovative ways of generating clean energy from a fast moving train. The three methods used include wind, solar and human excreta to generate energy. To tap the energy from wind, the turbine is installed on the train roof however for solar energy, the researchers here propose two methods, namely; installing solar panels on the roof or using roof materials integrated with solar cell modules. It's noted that integrating solar modules in the roof material reduces the mass per unit area as compared to installing solar panels on the roof. Also noted is that on average

as a rule of thumb, modern PV systems produce 8-10W per square foot of solar panel area [39].

2.5 Effect of Drag on Train Performance

The installation of the additional structure on the top of the train increases the air drag exerted, which in turn increases the power required in locomotive to overcome that extra drag force. Therefore, it is quite important to estimate the amount of drag and it is best to minimize it. The drag and lift forces depend on the density ρ of the fluid, the upstream velocity *V*, and the size, shape, and orientation of the body, among other things [30] [40];

$$F_d \ \frac{1}{2} C_d \rho V^2 A \qquad 2.14$$

Where A, is ordinarily the frontal area which is the area projected on a car normal to the direction of flow of the body, V is Velocity of air and ρ is the density of air and C_d is the drag coefficient.

The power needed to overcome this drag is given by;

$$W_d = F_d \times V \qquad 2.15$$

2.6 Effect of Additional Weight on Specific Energy Consumption of the train

Installing solar panels on the roof of the train increases its weight which in turn increases its energy consumption (EC). *Hinrich Helms et al, 2003*, estimated the energy consumption as a function of the weight for electric traction by the relation below [41];

$$EC_{train} \left[\frac{wh}{km}\right] = 315 * M_{train}[t]^{0.6} \qquad 2.16$$

Where;

EC_{train} = specific energy consumption per train-km

M_{train} = total gross weight of train in tones (t)

For a solar system to be effective, the amount of energy generated should be much more than the resulting increment in energy consumption as a result of the addition weight.

2.7 Optimization of Hybrid Renewable Energy Systems

The power produced from solar and Wind systems highly depends on the weather condition and this therefore makes them un-reliable since weather changes yearly. It's for this reason therefore that in most cases these two systems are combined, with some form of storage devices like batteries. This stored energy can be used in case there is no sufficient sunlight or wind speeds for electricity generation, therefore the optimal sizing of the different components is a crucial aspect of a hybrid renewable energy system [42].Various optimization techniques have been used and are shown in table 2-3 below.

Table 2-3: Various Optimisation techniques [42]

Optimization Techniques	**Optimized Elements**	**Remarks**
Graphical Construction	Battery and PV array	Normally used for two parameters
Probabilistic approach	Performance of hybrid-system	Based on statistical approach of data collection
Deterministic approach	Standalone PV with battery bank	Using equations for determining specific values using a constant parameters
Iterative approach a. Hill climbing b. Dynamic Programming c. Linear Programming d. Multi objective	Hybrid solar-wind system	Based on LPSP to find possible combination of solar-wind combination
Artificial Intelligence a. Genetic Algorithm b. Particle Swarm c. Fuzzy Logic d. Artificial Neural Network e. Hybrid model	Hybrid solar-wind system with battery bank	Based on Evolution technique

Optimization Techniques	Optimized Elements	Remarks
Software based a. HOMER		Input file with all necessary information is supplied. The software takes care of other things.

For this research, Hybrid Optimization Model for Multiple Energy Resources (HOMER) software was used for optimization. HOMER is a commercial software application developed by the National Renewable Energy Laboratory in the United States. This software application is used to design and evaluate technically and financially the options for off-grid and on-grid power systems for remote, stand-alone and distributed generation applications. It allows you to consider a large number of technology options to account for energy resource availability and other variables. The software is easy to use, allows multiple energy sources to be optimized and also does a sensitivity analysis. It has also been used by over 150,000 people in 193 countries. It's for these reasons that this software was used for this research [43].

2.8 Conclusion

Previous studies have been done on green energy in railway however no optimal method has been obtained. Therefore, this research aims at determining the optimal method of generating solar and wind energy in railways using AALRT as a case study. The power generated can either be used to power the auxiliary systems or even supply the motive power needed if generated in sufficient quantities.

CHAPTER 3 METHODS, DATA COLLECTION AND PRELIMINARY CALCULATIONS

3.1 Introduction

This chapter covers the details of the methods that were used in this research. Below is the flow diagram that to describe the methods undertaken.

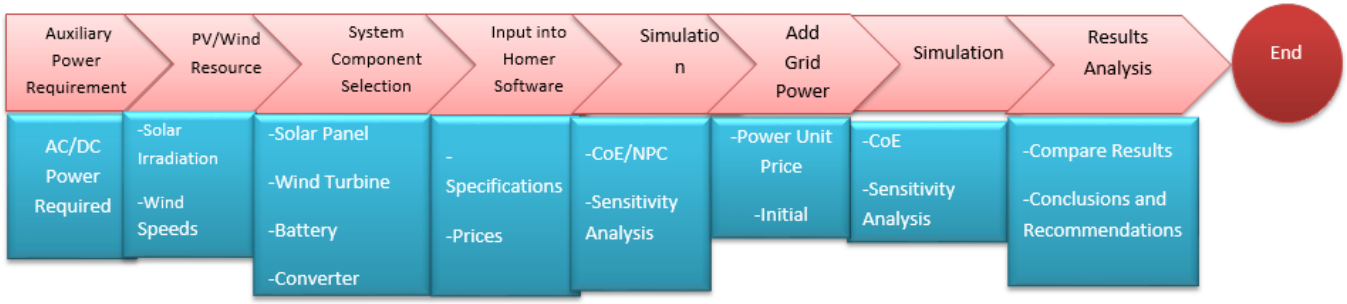

Figure 3-1: Flow Diagram Showing the Methods used

3.2 Auxiliary Power Supply system for Multiple Units at AALRT

The auxiliary power supply system includes auxiliary inverter and batteries. Auxiliary inverter supplies AC380V and DC24V to vehicles and charges the batteries. When high input voltage of DC 750V is not available (auxiliary inverter not working) for vehicles, it also supplies vehicles with control power and emergency power supply. It has two systems namely, AC and DC power supply systems [44].

3.2.1 Auxiliary AC power supply

It has the following specifications;

Rated capacity - 35kVA

Input Voltage – DC 750V

Range of Voltage – DC 500V – 900V

Output Voltage – 3-phase 380V and single phase 220V

Output frequency- 50Hz ± 1%

3.2.2 Auxiliary DC power supply

Main electrical parameters for the charger;

Output power: 12V/8kW
Accuracy of voltage: 12V±3%
Ripple coefficient: < 5%

3.3 Solar Energy Assessment for Addis Ababa

The solar radiation assessment for Addis Ababa was done by collecting data from two different sources, namely; National Metrological Service Agency of Ethiopia (NMSA) and National Aeronautics and Space Administration (NASA). This was done to ensure the accuracy of data from both sources as opposed to relying on data from one source.

The data recorded at NMSA is daily sunshine hours and therefore the mathematical approach as explained previously was used to estimate the solar radiation. The regression

coefficients as obtained by Drake and Mulugeta (1996), for different regions of Ethiopia were used i.e. a = 0.191 and b = 0.622 [24]. The data collected is summarized in table 3-1 below and is presented in Appendix A. The missing data wasn't recorded by the agency.

Table 3-1: Average Monthly Sunshine hours obtained from NMSA

	Jan	**Feb**	**Mar**	**Apr**	**May**	**June**	**July**	**Aug**	**Sept**	**Oct**	**Nov**	**Dec**
2016	7.4	9.1	7.6	-	5.7	4.1	-	2.6	4.4	7.5	7.8	9.4
2017	10	7.9	8.2	8.4	-	5.4	2.4	2.8	3.7	-	8.9	9.8
2018	8.3	8.6	7.1	7.8	6.7	5.5	3.8	2.9	-	6.7	8.1	9.5
Average Sunshine hrs	**8.6**	**8.5**	**7.6**	**8.1**	**6.2**	**5.0**	**3.1**	**2.8**	**4.1**	**7.1**	**8.3**	**9.6**

Using the mathematical approach in Appendix C, the results obtained are shown in table 3-2.

Table 3-2: Estimated Solar Radiation

Month	**Solar Radiation, kW/h/m^2/day**			
	2016	**2017**	**2018**	**Average**
Jan	5.4	6.7	5.9	6.0
Feb	6.6	6.0	6.4	6.3
Mar	6.2	6.5	5.9	6.2
Apr	2.1	6.7	6.4	5.1
May	5.1	2.1	5.7	4.3
June	4.2	4.9	5.0	4.7
July	2.1	3.4	4.1	3.2
Aug	3.5	3.6	3.7	3.6
Sept	4.5	4.1	2.1	3.5
Oct	5.9	1.9	5.5	4.5
Nov	5.7	6.3	5.9	6.0
Dec	6.3	6.5	6.3	6.3

To be able to ensure accuracy of the data from NMSA, the corresponding data from NASA was also obtained for comparison purposes. The data obtained is shown in table 3-3.

Table 3-3: Solar radiation obtained from NASA [45]

	Jan	**Feb**	**Mar**	**Apr**	**May**	**June**	**July**	**Aug**	**Sept**	**Oct**	**Nov**	**Dec**
2016	6.3	6.6	7.1	7.5	7.4	7.3	6.6	7.2	6.8	-	6.8	6.6
2017	6.1	6.8	7.5	7.8	7.5	7.0	6.9	-	-	6.7	6.7	6.5
2018	6.4	6.9	7.3	7.4	7.3	7.1	-	6.7	7.2	6.9	6.5	6.3
Average Solar radiation kWh/m^2/day	**6.3**	**6.8**	**7.3**	**7.6**	**7.4**	**7.1**	**6.75**	**6.9**	**7.0**	**6.8**	**6.7**	**6.5**

The data from both sources seems to agree however the biggest discrepancy is because some of the data wasn't captured in both sources. All in all, the data implies that Addis Ababa has a good potential for solar energy with radiation values ranging from 4kWh/m^2/day to 7kWh/m^2/day. This is the radiation on a horizontal surface. Considering that the roof of the train is also flat as shown in figure 3-2, then the collected data should suffice.

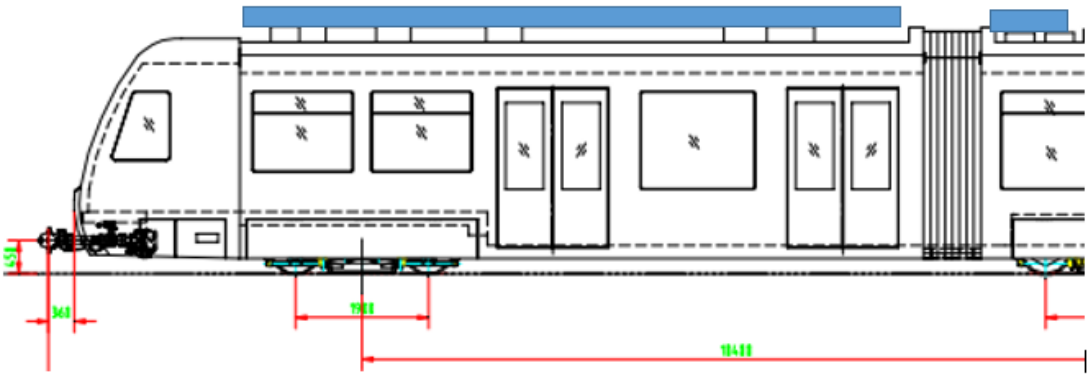

Figure 3-2: Section of the train showing where the solar panels (in blue) shall be installed

3.4 Calculating available roof space

Each multiple unit at AALRT has two Motor cars and 1 trailer car (2M1T). The available space on each Motor Car is 11.3 x 2.65 = 29.9 m^2. This makes it 59.8 m^2 as the total surface area available for the motor cars.

The trailer car hosts the pantograph and therefore has a reduced available surface area which is approximately 0.9 x 2.65 = 2.385 m^2. Therefore, the total available rooftop area for each unit is 62.2 m^2 [44].

3.5 Estimating the number of solar panels

Considering the maximum rated solar panel available on the Ethiopian market which is rated 300W and dimensions (195.59 X 99.06) mm [46], giving a total area of 1.937 m^2. Therefore, the number of solar panels that can be installed on each unit is 32 panels.

However, when these panels are fixed on the rooftop and a spacing of 0.25m is allowed between panels, only 21 panels can fit. Figure 3-3 shows the panels that can fit on one Motor car and one trailer car. Considering that a full unit is 2M1T, then the total number of solar panels that can fit is 21 panels. Therefore, the total area covered by the solar panels is 41.5 m^2.

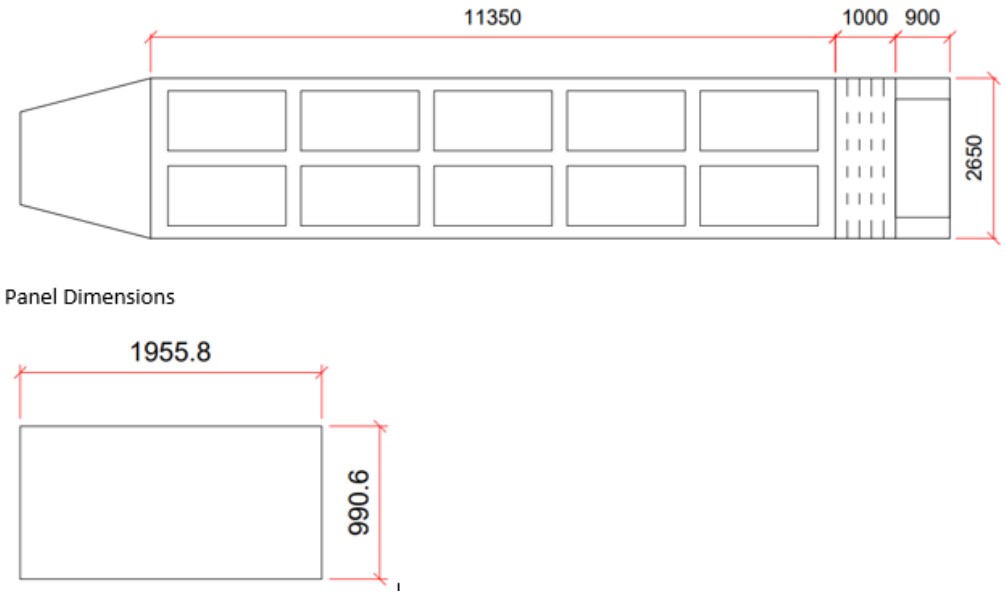

Figure 3-3: Scale drawing showing solar panels configuration on Motor and Trailer Car

3.6 Power output from PV panels

Using equation 2.13, and considering the average incident solar radiation, G_T = 4.7kWh/m^2/day, the average amount of power that can be generated is 24.6kWh/day.

The auxiliary system at AALRT has constant voltage of 12V DC, therefore these solar panels have to be connected in parallel to be able to meet this requirement. Parallel connection ensures same voltage and increased current whereas series connection ensures increased voltage and same current. The connection is shown in figure 3-4 below;

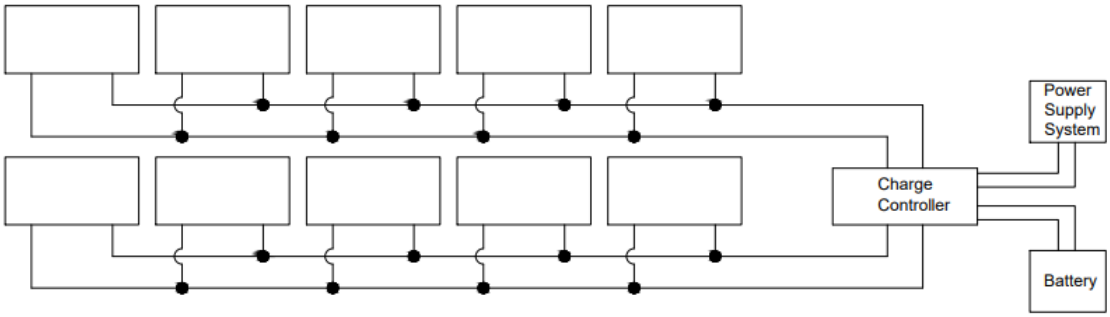

Figure 3-4: Parallel connection of the solar panels

3.7 Battery Sizing

Each multiple unit at AALRT has 2 x 60Ah, Ni-Cd battery with rated voltage 1.2V/cell. According to the manual, the battery should be sized to retain door control, emergency lighting, external lighting, train borne safety devices, PA and communications in operation for duration of not less than 30 minutes in case of vehicle failure [44]. If the solar system is selected to be used, then the battery should be sized to run the system for atleast 6 hours of the day when there is no sunlight i.e from 6am to 9am and 7pm to 9pm daily. However if wind energy is selected, then the battery should be sized as per the manufacturer's recommendation because there will always be wind as long as the train is in motion. For the solar system, the battery sizing should be done based on the procedure below.

To determine the optimal battery sizing, the following method shall be used [46];

- Total Watt-hours per hour needed = 8,000 Watt
- Divide the total Watt-hours per hour used by 0.85 for battery loss= 8,000/0.85= 9,411.8W
- Divide the answer obtained above by 0.6 for depth of discharge= 9,411.8W /0.6 = 15,686.3W
- Divide the answer obtained above by the nominal battery voltage = 15,686.3W/7.2 = 2178.7A
- Multiply the answer obtained above with hours of autonomy (the number of hours that you need the system to operate when there is no power produced by PV panels) to get the required Ampere-hour capacity of deep-cycle battery = 2178.7* 6 hours = 13071.9Ah
- The above procedure can be summarised as below:

$$\textbf{Battery Capacity (Ah)} = \frac{\textbf{Total Watt-hours per day needed x hours of autonomy}}{(\textbf{0.85 x 0.6 x nominal battery voltage})} \quad \textbf{3.1}$$

Considering the specifications of the batteries already installed on the units i.e. Ni-Cd 2 x 60Ah and 1.2 v/ cell, the number of similar batteries required to supply power to the auxiliary system for about 6 hours when there is no sunlight is 218 batteries. This is quite a big number and considering the limited space available on the rooftop and the effect of this additional weight on train performance, this ought to be reduced drastically. This can be done by either of the following ways.

There are different battery sizes available on the market and currently manufactures can customize the battery size depending on the different needs [47]. Therefore, to come up with the optimal sizing of the battery, the manufacturers can be contacted to customize the battery for this specific application and this would mean changing the batteries already installed on the units.

Alternatively, the batteries available on the units can be used to run the systems for atleast 30 minutes as per the manufacturer's recommendations [44]. This would favor both the wind and solar systems and more cost effective since the batteries don't have to be changed.

3.8 Charge Controller sizing

The charge controller is an essential part of the solar system. It protects the battery against both excessive overcharge and deep discharge. Charge controller switches off the load when a certain state of discharge is reached, it also switches off battery from the DC bus when it is fully charged. It can be designed to deal with different charge and discharge conditions. So the charge controller is modelled by its efficiency where the output is given by [48];

$$P_{PVR} = P_{pv\,out} * \eta_{PVR} \quad 3.2$$

Where:

P_{PVR} is output of the power PV controller.
P_{PVout} is the PV panel power output
η_{PVR} is the efficiency of the PV charge controller

Considering the efficiency of the charge controller as 90% [49], the charge controller for this case should be rated 24.6kW * 0.9 = 22.1kW or higher.

3.9 Inverter Sizing

The auxiliary power supply system for multiple units at AALRT has both the DC and AC supply. This implies that the part of the DC generated from the PV cells should be converted to AC to meet this demand. Each unit is installed with auxiliary inverter control unit for output of logic control signal of auxiliary power supply system, to control the operations of auxiliary inverters and charger, to respond to all operation commands and to execute controlled operations of auxiliary power supply system based on special characteristics Auxiliary inverter supplies AC380V and DC24V to vehicles and charges the batteries. [44]. This is the inverter size that was used in the simulation.

3.10 Effect of the additional weight on energy consumption

On average, solar panels and mounting equipment weigh 10-20 kg per square meter [50]. Considering an average value of 15kg/m^2, with 41.5m^2 of solar panels, this means the total addition weight is 622.5kg.

Using equation 2.16, the resulting increment in specific energy consumption is 59.9 Wh/km. Each line at AALRT is 17km, therefore the resulting increment in energy consumption per trip is 1kWh and if each unit makes 13 trips in a day, this means the resulting energy increament is 13kW per day, considering that we are able to produce 24.6kWh/day, this implies that out net energy generated is 11.6kW.

3.11 Wind Potential Assessment of Addis Ababa

The wind resource assessment for Addis Ababa was obtained from NASA as shown in table 3-5 and table 3-6. Though a lot of data wasn't captured at NMSA and therefore the complete data was obtained from NASA. Comparing the 2 sets of data, they seem to be in agreement since the higher the height of measurement the higher the wind speed [48]. NMSA measures wind speed at height of 5m whereas NASA measures wind speed at height of 10m. The data collected is presented below;

Table 3-4: Average Wind speed (m/s) measured at height of 10m from NASA [45]

	Jan	Feb	March	April	May	June	July	Aug	Sept	Oct	Nov	Dec
2016	2.7	2.66	2.97	2.28	2.56	2.39	2.54	2.41	2.10	2.55	2.70	2.80
2017	2.34	2.87	2.73	2.95	2.38	2.67	2.16	2.36	1.96	2.76	2.27	2.33
2018	2.37	2.73	2.71	2.25	2.82	2.31	2.22	2.39	2.21	2.79	3.12	2.36

Table 3-5: Average Wind speed (m/s) measured at a height of 5m obtained from NMSA

	Jan	Feb	March	April	May	June	July	Aug	Sept	Oct	Nov	Dec
2016	0.8	0.9	0.9	0.6	0.6	0.5	0.5	0.4	0.5	0.6	0.7	0.7
2017	0.6	0.7			0.6			0.3	0.4		0.6	
2018												

The minimum wind speed for a wind turbine to be able to produce power normally is about 3m/s [51] [23] depending on the type of turbine. With the above wind speeds, there would be no power that can be produced by the wind turbine.

However, when the vehicle is moving at a high speed, it induces the wind speed that is higher than the ambient wind speed. Due to limited resources, I was unable to measure the induced wind speeds on the trains at AALRT. I therefore used the existing literature to estimate the wind speeds.

Habib Nasser, 2013 [33], carried out a study on the induced wind speeds when the vehicle is in motion. He fixed a wind turbine on top of the car and recorded the data when the vehicle was moving at different speeds of 30, 50, 70 and 90km/h. The results obtained were plotted and shown on graphs as in figure 3-5.

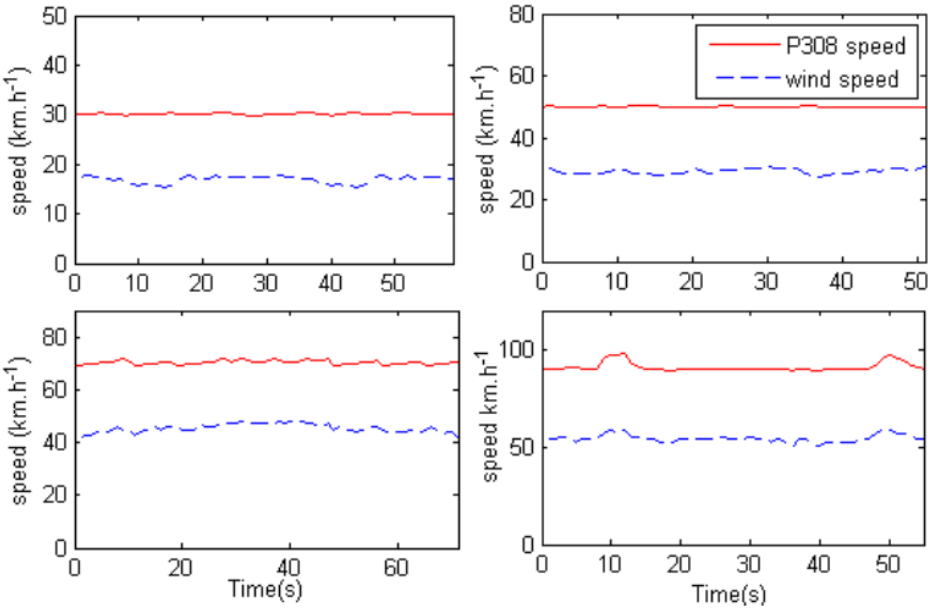

Figure 3-5: Vehicle and wind speeds at 30, 50, 70 and 90km/h [15]

As can be observed, the induced wind speed is always less than the actual vehicle speed by approximately 50%.

Shan Varghese Abraham, 2018 [52], carried out a similar experiment and the results are presented in figure 3-6 below;

Sl No	*RELATION BETWEEN SPEED OF VEHICLE AND WIND PRODUCED*		
	VEHICLE SPEED(km/hr)	*TORQUE*	*WIND SPEED m/s*
1	*20*	*10*	*2*
2	*30*	*17*	*7*
3	*40*	*22*	*9*
4	*50*	*32*	*11*
5	*60*	*42*	*14*
6	*70*	*52*	*15*

Figure 3-6: Relation between wind speed and vehicle speed [52]

Converting vehicle speed from km/h to m/s, the results in table 3-1 are obtained;

Table 3-6: Correlation between vehicle speed and wind speed

Sl No	Vehicle Speed(m/s)	Wind Speed(m/s)
1	5.6	2
2	8.3	7
3	11.1	9
4	13.9	11
5	16.7	14
6	19.4	15

As can be observed from table 3-1, the induced wind speed is slightly less than the vehicle speed but by a smaller difference as compared to figure 3-5. The induced wind speed depends on a number of factors, among others that include;

- the ambient wind speed
- the direction of the wind

This could partly explain the difference in the two results obtained. From this literature, it can thus be concluded that the induced wind speed is normally slightly less than the vehicle speed. For purposes of this project, the worst case scenario was considered i.e. the vehicle speed is two times higher than the induced wind speed as in figure 3-5.

At AALRT, the minimum speed is 0 km/h and the maximum speed is 30km/hr. This translates to 0m/s to 8.3m/s respectively. The train driver decides on what speed to cruise at depending on the length of the section and if there are any pedestrian crossings in that section however when the maximum speed is reached, emergency brakes are automatically applied.

Considering the worst case scenario as explained above, implies that at maximum speed, the induced wind speed is about 4m/s. This wind speed is too low to produce reasonable wind energy and therefore has to be boosted. It's thus recommended to place the turbine in a conical duct to improve the speed of the wind hitting the turbine and increasing power production in due course.

3.12 Wind Turbine

The kinetic energy of the wind is used the driving force of wind turbine. Under the constant acceleration, the kinetic energy of the wind can be depicted by equation 3.3 below [53] [52] [33];

$$E = \frac{1}{2}mv^2 \quad 3.3$$

Where,

E = the kinetic energy (J)
m = the mass (weight) of air (Kg)
v = the velocity of the wind (m/s)

So, kinetic energy in the wind per second which is equal to power (P) in the wind in watts is equal to;

$$P = \frac{1}{2}\rho A v^3 \quad 3.4$$

Where;

P is power in watts (W)
ρ is the air density in kilograms per cubic meter (kg/m^3)
A is the swept rotor area in square meter (m^2)
V is the wind speed in meter per second (m/s) [53] [52] [33].

Since the breadth of the multiple units at AALRT is 2650mm or 2.65m [44], the maximum possible radius of the wind turbine is 1m. The swept area, A = r^2 , r=1m, and therefore A= 3.142m^2

Considering wind speed as 4m/s and the density of air as 1.23Kg/m^3, the maximum amount of power that can be generated is 123W.

A German physicist Albert Betz concluded in 1919 that no wind turbine can convert more than 59.3% of the kinetic energy of the wind into mechanical energy to turn a rotor. This is known ad Betz limit .This is called power coefficient C_p. [29]. If this coefficient is factored in, then the actual amount of power that can be generated is 73.3W.

If we take into account the other factors in a complete wind turbine system e.g. the gearbox, bearings, generator, and mechanical loading effect and so on, the power available is further reduced.

Such an amount of power generation is not worth the investment. Since the amount of power generated is highly dependent on the wind speed as shown in equation 2.7, then measures have to be put in place to increase it. One of the ways this can be done is to place the wind turbine in a conical duct, the duct is designed as a converging nozzle at the entrance and a diverging nozzle at the exit to reduce the drag as the wind is exiting.

3.12.1 Design of the conical duct

The duct is designed in such a way as to sit on the section of the roof that is shaded blue in figure 3-7. This section measures (4030 x 2650) mm. The thickness of the duct is made as small as possible to minimize the effect of drag, this thickness is assumed to be 20mm.

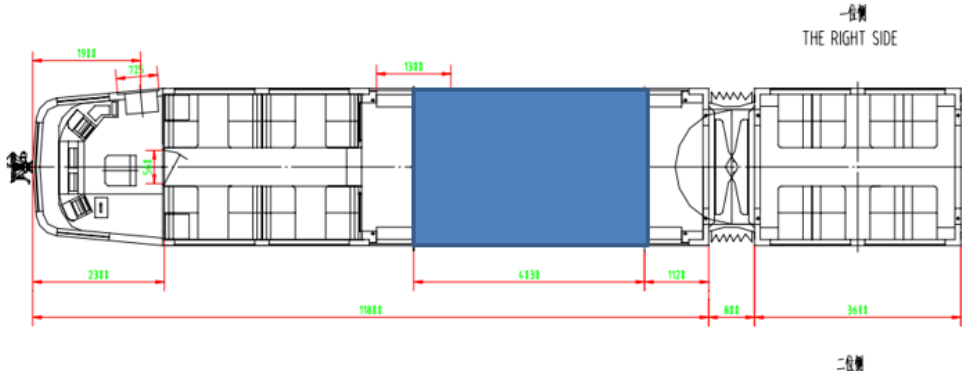

Figure 3-7: Position of duct and wind turbine (in blue)

The Area of the inlet is $l_1 \, x \, b_1$, where $l_1 = 2.65m$ and the Area of the exit is $l_2 \, x \, b_2$, and $b_1 = b_2$.

From the continuity equation,

$$A_1V_1 = A_2V_2 \qquad 3.5$$

The Velocity at the inlet V_1 = 4m/s as explained previously, and the desired speed at the turbine V_2 = 15m/s which is the assumed rated output speed of the turbine.

Equation 3.6 can be expanded to become;

$$L_1b_1V_1 = L_2b_2V_2 \qquad 3.6$$

Substituting the known variables gives and L_2 = 0.71m. Therefore, to obtain atleast 15m/s wind speed hitting the turbine, the entry side of the duct should be 2.65m and the exit to the turbine should be 0.71m. The proposed conical duct looks as in figure 3-8,

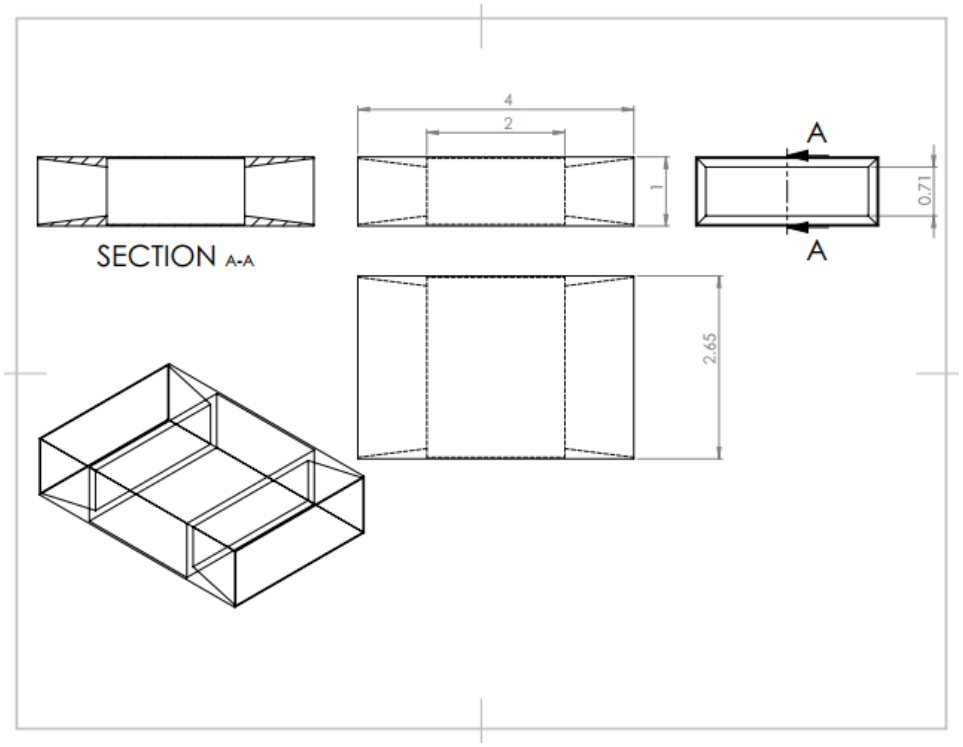

Figure 3-8: Proposed conical duct

With the addition of the duct, the amount of energy that can be generated considering wind speed of 15m/s is 3.8kW by using equation 3.4 and also considering the Betz limit, C_p. The designed turbine has a power curve as shown below

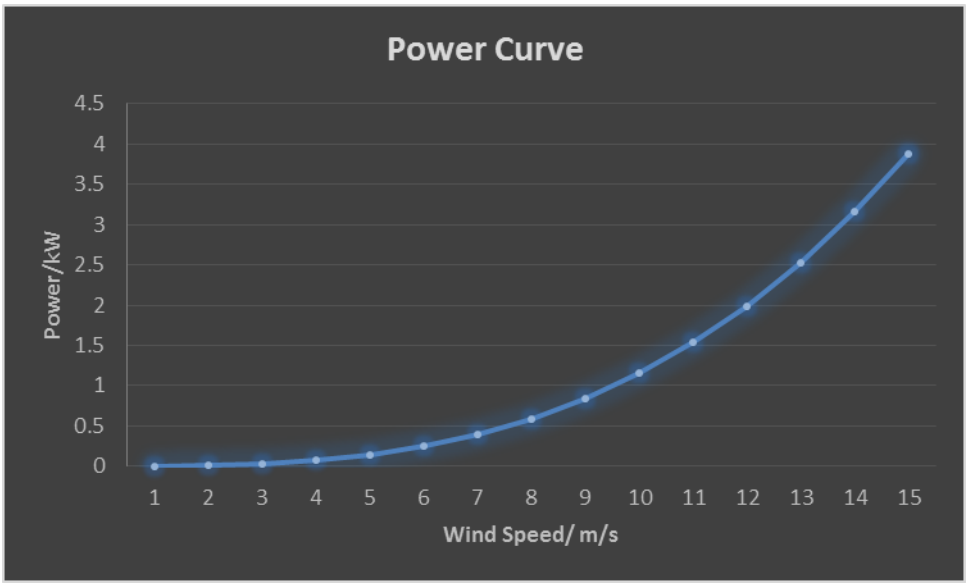

Figure 3-9: The designed wind turbine power curve

From the curve, it can be deduced that the cut in wind speed of this turbine is 5m/s and the rated wind speed is 25m/s.

To be able to simulate this in HOMER software, the projected wind speeds have to be distributed annually since the software considers average monthly wind speeds. Since the train drivers at AALRT have no defined speed profiles, it's assumed at each time of the day, the turbine will experience all the wind speeds from the minimum up to the maximum. These can be averaged to a monthly basis. The projected wind speeds are shown in table 3-2.

Table 3-7: Assumed Induced wind speeds (m/s)

	Jan	Feb	March	April	May	June	July	Aug	Sept	Oct	Nov	Dec
2016	4.0	5.0	6.0	7.0	8.0	9.0	10.0	11.0	12.0	13.0	14.0	15.0

3.12.2 Effect of drag on train performance

Installing a wind turbine on the roof train has effects on train performance. One is the resulting drag which affects the train aerodynamics leading to a higher specific energy consumption. The other is the addition weight which also results in increased energy consumption however in most cases, the additional weight is negligible and therefore the resulting increament in energy is also negligible. Therefore, the biggest setback is the resulting drag [46].

Using equation 2.14, and substituting the following variables; the density of air $\rho = 1.236$ kg/m^3, velocity of wind at the inlet to the duct as 15m/s, the swept area, A of the turbine is 3.142m^2, the drag coefficient of the turbine is estimated from the figure 3-9 below;

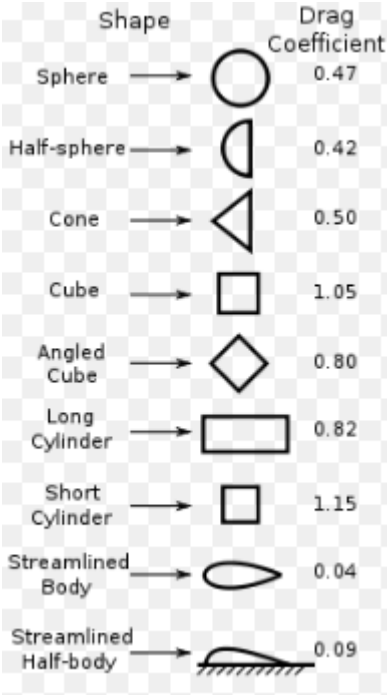

Figure 3-10: Measure drag coefficients for different shapes [54]

Considering the wind turbine blades to be a streamlined body, the power of coefficient is C_d= 0.04. Therefore, the resulting drag force, F_d = 5.562N.

The power W_d needed to overcome this drag, using equation 3.10 is 83.43W. Considering that we are able to produce 3.8kW by this turbine, then this investment is worthwhile.

3.12.3 Hybrid power generation system

A hybrid system is a combination of one or more resources of renewable energy such as solar, wind, micro/mini-hydropower and biomass with other technologies such as batteries and diesel generator. As an off-grid power generation, the hybrid system offers clean and efficient power that will in many cases be more cost-effective than sole diesel systems. As a result, renewable energy options have increasingly become the preferred solution for off-grid power generation [55] [56].

This research also explored the possibility of having a pv/wind hybrid system installed on the rooftop as an alternative to hydro power that is used for the auxiliary power system. Hybrid wind turbine and PV modules, offer greater reliability than any one of them alone because the energy supply does not depend entirely on any one source. For example, on a cloudy stormy day when PV generation is low there's likely enough wind energy available to make up for the loss in solar electricity, and as a result the size of the battery storage can be reduced [13].

Wind and solar hybrids also permit use of smaller, less costly components than would otherwise be needed if the system depended on only one power source. This can substantially lower the cost of a power system. In a hybrid system, the designer doesn’t need to weigh the components for worst-case conditions by specifying a larger wind turbine and battery bank than is necessary [13].

Other advantages of the hybrid system are the stability and immobility of the system and a lower maintenance requirement, thus reducing downtime during repairs or routine maintenance. In addition to this, as well as being indigenous and free, renewable energy resources also contribute to the reduction of emissions and pollution [57].

CHAPTER 4 DESIGNING AND MODELLING OF HYBRID SYSTEM WITH HOMER

4.1 Overview

The Hybrid Optimization Model for Electric Renewables (HOMER), which is copyrighted by Midwest Research Institute (MRI) is a computer model developed by the U.S. National Renewable Energy Laboratory (NREL) to assist the design of power systems and facilitate the comparison of power generation technologies across a wide range of applications [58].

HOMER is used to model a power system physical behavior and its life-cycle cost, which is the total cost of installing and operating the system over its life time. HOMER allows the modeler to compare many different design options based on their technical and economic merits. It also assists in understanding and quantifying the effects of uncertainty or changes in the inputs [58].

HOMER performs three principal tasks: simulation, optimization, and sensitivity analysis based on the raw input data given by user. In the simulation process, the performance of a particular power system configuration for each hour of the year is modeled to determine its technical feasibility and life-cycle cost. In the optimization process, many different system configurations are simulated in search of the one that satisfies the technical constraints at the lowest life-cycle cost. In the sensitivity analysis process, multiple optimizations are performed under a range of input assumptions to judge the effects of uncertainty or changes in the model inputs. Optimization determines the optimal value of the variables over which the system designer has control such as the mix of components that make up the system and the size or quantity of each. Sensitivity analysis helps assess the effects of uncertainty or changes in the variables over which the designer has no control, such as the average wind speed or the future fuel price [58].

4.2 Simulation

The simulation process determines how a particular system configuration, a combination of system components of specific sizes, and an operating strategy that defines how those components work together, would behave in a given setting over a long period of time.

HOMER can simulate a wide variety of micropower system configurations, comprising any combination of a PV array, one or two wind turbines, a run-of-river hydro-turbine, and up to three generators, a battery bank, a dc-ac converter, an electrolyzer, and a hydrogen storage tank. The system can be grid-connected or autonomous and can serve ac and dc electric loads and a thermal load [58].

The simulation process serves two purposes. First, it determines whether the system is feasible. The feasible system is one which can adequately serve the electric and thermal loads and satisfy any other constraints imposed by the user. Second, it estimates the life-cycle cost of the system, which is the total cost of installing and operating the system over its lifetime. The lifecycle cost is a convenient metric for comparing the economics of various system configurations.

A particular system configuration is modeled by performing an hourly time series simulation of its operation over one year. Simulation steps through the year one hour at a time, calculating the available renewable power, comparing it to the electric load, and deciding what to do with surplus renewable power in times of excess, or how best to generate additional power in times of deficit. When one year's worth of calculations is completed, it is determined whether the system satisfies the constraints imposed by the user on such quantities as the fraction of the total electrical demand served, the proportion of power generated by renewable sources, or the emissions of certain pollutants, etc. The quantities required to calculate the system's life-cycle cost, such as the annual fuel consumption, annual generator operating hours, expected battery life are also computed [58].

The quantity used to represent the life-cycle cost of the system is the total net present cost (NPC). This single value includes all costs and revenues that occur within the project lifetime, with future cash flows discounted to the present. The total net present cost includes the initial capital cost of the system components, the cost of any component replacements that occur within the project lifetime, the cost of maintenance and fuel.

4.3 Optimization

The simulation process models a particular system configuration, whereas the optimization process determines the best possible system configuration. The best possible, or optimal,

system configuration is the one that satisfies the user-specified constraints at the lowest total net present cost. Finding the optimal system configuration may involve deciding on the mix of components that the system should contain, the size or quantity of each component, and the dispatch strategy the system should use. In the optimization process, many different system configurations are simulated; the infeasible ones are discarded, the feasible ones are ranked according to total net present cost, and the feasible one is presented with the lowest total net present cost as the optimal system configuration [58].

The goal of the optimization process is to determine the optimal value of each decision variable that interests the modeler. A decision variable is a variable over which the system designer has control and for which multiple possible values can be considered in the optimization process. Possible decision variables include;

- The size of the PV array
- The number of wind turbines
- The size of each generator
- The number of batteries
- The dispatch strategy

Optimization can help the modeler find the optimal system configuration out of many possibilities. Multiple values for each decision variable can be entered in search space, which is the table that contains the set of all possible system configurations over which HOMER can search for optimal system configuration. In the optimization process, every system configuration in the search space is simulated and the feasible ones are displayed in a table, sorted by total net present cost.

4.4 Sensitivity Analysis

In the sensitivity analysis process multiple optimizations are performed, each using a different set of input assumptions. A sensitivity analysis reveals how sensitive the outputs are to changes in the inputs. In a sensitivity analysis, a range of values for a single input variable are fed to HOMER. A variable for which the user has entered multiple values is called a sensitivity variable. Almost every numerical input variable that is not a decision variable can be a sensitivity variable. Examples include, the PV module price, fuel price, interest rate, etc.

A sensitivity analysis can be performed with any number of sensitivity variables. Each combination of sensitivity variable values defines a distinct sensitivity case. A separate optimization process for each sensitivity case is performed and the results are presented in various tabular and graphic formats.

One of the primary uses of sensitivity analysis is in dealing with uncertainty. If a system designer is unsure of the value of a particular variable, he/she can enter several values covering the likely range and see how the results vary across that range. But sensitivity analysis has applications beyond coping with uncertainty. A system designer can use also sensitivity analysis to evaluate trade-offs between different options.

4.5 Hybrid System Modelling

This section describes how HOMER models the physical operation of a system in greater detail. A power system must comprise at least one source of electrical or thermal energy (such as a wind turbine, a diesel generator, or the grid), and at least one destination for that energy (electrical or thermal load). It may also comprise conversion devices such as a dc-ac converter or an electrolyzer, and energy storage devices such as a battery bank or a hydrogen storage tank.

The following subsections are devoted to how to model the loads that the system must serve, the components of the system and their associated resources, and how that collection of components operates together to serve the loads.

4.5.1 Electrical Loads

The electric loads are usually the largest single influence on the size and cost of hybrid system components. So, deciding on the loads is one of the most important steps in the design of the hybrid system. The term loads refers to a demand for electric or thermal energy, if any. Three types of loads can be modeled using HOMER: primary load which is electric demand that must be served according to a particular schedule, deferrable load which is electric demand that can be served at certain period of time, the exact timing is not important and thermal load which is demand for heat.

Primary Load: Primary load is electrical demand that the power system must meet at a specific time. If electrical demand exceeds supply, there is a deficit that is recorded as unmet load.

Deferrable Load: Deferrable load is electrical demand that can be met anytime within a certain time span, and the exact timing is not important.

In this thesis, all auxiliary services were considered to be primary load since the main objective was to supply power to meet the specifications of the auxiliary power supply system.

4.5.2 Economic Modelling

The main objective of this research is to find an optimal method of generating power from the train rooftop to supply power for the auxiliary systems. The optimal method shall be selected based on the total Net Present Cost and energy cost. HOMER computes the following cost analysis;

a. *Net Present Cost (NPC):* NPC indicates the installation cost and the operating cost of the system throughout its lifetime which is calculated as follows [59];

$$NPC = \frac{TAC}{CRF(i,Rprj)} \quad 4.1$$

Where, TAC, CRF, i and Rpr_j are Total Annualized Cost ($), Capital Recovery Factor, interest rate in percentage and project life time in year respectively.

b. *Total annualized cost:* It is the sum of the annualized costs of every equipment of the power system including capital and operation and maintenance cost. It also includes replacement and fuel cost [59].
c. *Capital recovery factor:* It is a ratio which is used to calculate the present value of a series of equal annual cash flows [59];

$$CRF = \frac{i\,x\,(1+i)^n}{(1+i)^{n-1}} \quad 4.2$$

Where, *n* and *i* represents the number of years and the annual real interest rate, respectively.

d. *Annual real interest rate:* It is a function of the nominal interest rate shown as below [59].

$$i = \frac{i^1-F}{1+F} \quad 4.3$$

1.1 Where, *i*, *i'* and F is the real interest rate, nominal interest rate, and annual inflation rate, respectively.

e. *Cost of energy (COE):* It is the average cost/kWh of useful electrical energy produced by the system. The COE is calculated as follows [59].

$$COE = \frac{TAC}{L_{prim,AC} + L_{prim,DC}} \quad 4.4$$

Where, $L_{prim,AC}$ *and* $L_{prim,DC}$ are the AC primary load and the DC primary load, respectively

4.6 Input into the software

4.6.1 Modelling Wind Turbine

HOMER has a database with different wind turbines and their associated costs. From the calculations above, it was found out that the maximum amount of power that can be generated is 3.8kW. Therefore, a turbine that is able to generate this amount of power was selected from the HOMER database and with the almost a similar characteristic power curve as shown in figure 3-9 was selected.. The generic 3kW was selected, its capital and replacement costs are USD 18,000 and O&M cost is USD 180/year. The power curve is defined by the following;

- *Cut-in-speed:* is the wind speed at which the turbine starts to generate power.
- *Rated speed:* is the wind speed at which the turbine reaches rated turbine power.
- *Cut out speed:* the wind speed at which the wind turbine is shutdown to keep loads and generator power from reaching damaging levels.

The power curve of the selected turbine is shown in figure 4-1. The cut in wind speed is 5m/s and the rated speed is 15m/s.

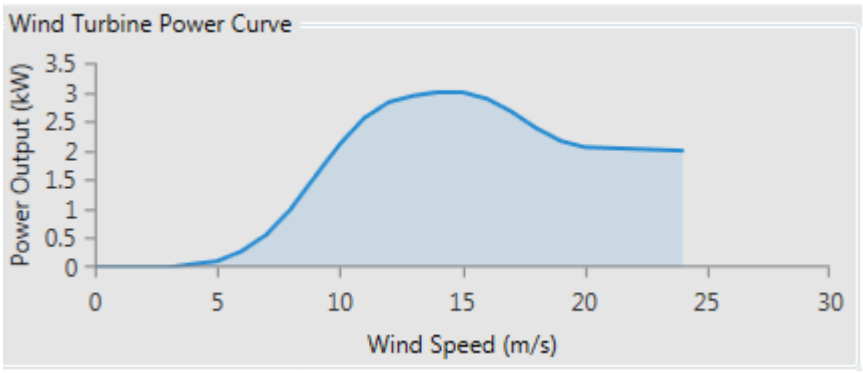

Figure 4-1: Turbine Power Curve

The wind speeds in Table 3-2 were fed in HOMER and are represented in figure 4-2.

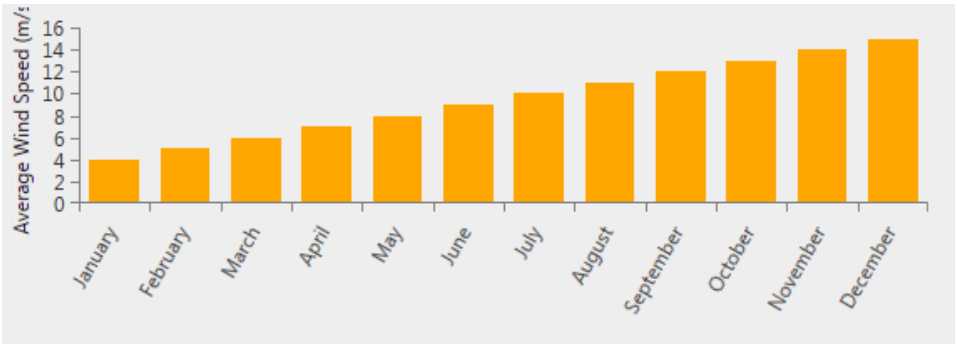

Figure 4-2: Average wind speeds as fed in HOMER

4.6.2 Modeling the Solar PV system

A 300W solar panel on the Ethiopian market costs around 9800 ETB (326USD), and with all the accessories and labor, it can go to as high up as 35000ETB(1100USD) [46]. This means 32 solar panels would cost 35,200USD. To simulate in HOMER, a solar panel that meets these specifications was selected and is the Jinko Eagle PERC 60 300W. The project lifetime is 25 years.

The solar resource for Addis Ababa entered in the system was downloaded from NASA surface meteorology and Solar Energy database averaged over a 22 year period. These values agree with the data obtained in Table 3-1. HOMER represents the data as in figure 4-3.

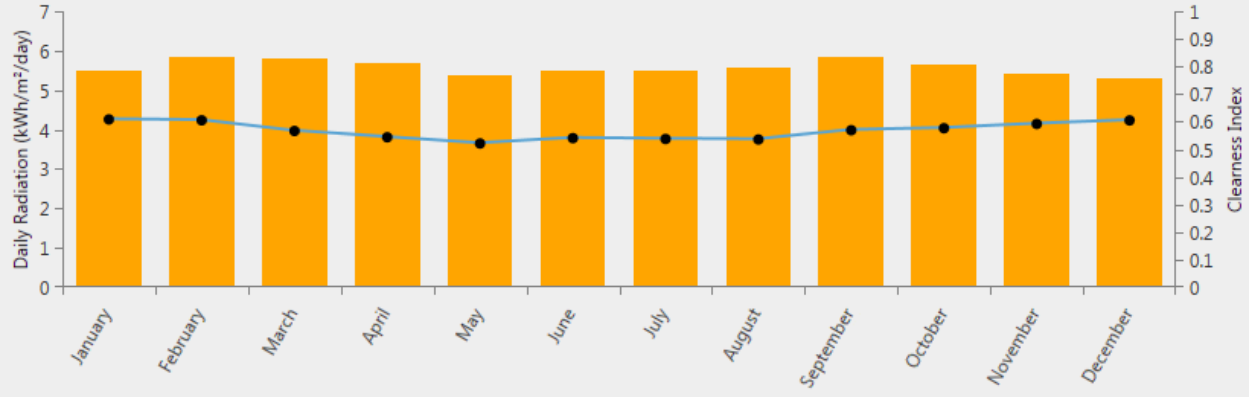

Figure 4-3: Monthly Solar Radiation and Clearness Index for Addis Ababa

The clearness index is a measure of the clearness of the atmosphere. It is the fraction of the solar radiation that is transmitted through the atmosphere to strike the surface of the earth. It is a dimensionless number between 0 and 1, defined as the surface radiation divided by the extraterrestrial radiation.

4.6.3 Battery

The power generated by the solar system needs to be stored in batteries for use when there is no sunlight or when the wind power is not sufficient to run the systems. Battery should be sized to retain door control, emergency lighting, external lighting, train borne safety devices, PA and communications in operation for duration of not less than 30 minutes in case of vehicle failure [44]. The units at AALRT have 2 x 60Ah, Ni-Cd battery, and rated voltage 1.2V/cell. To simulate this in HOMER, a Ni-Cd battery with the following specifications is selected from the database.

Nominal Voltage (V): 7.2
Nominal capacity (kWh): 0.12
Nominal capacity (Ah): 120
Roundtrip efficiency (%): 85
Maximum charge current (A): 1
Maximum discharge current (A):50

Homer estimates the capital cost and the replacement cost as USD 97 and the O&M cost as USD 0.25/year.

4.6.4 Converter

A converter is a device that converts electric power from dc to ac in a process called inversion, and/or from ac to dc in a process called rectification. The converter size, which is a decision variable, refers to the inverter capacity, meaning the maximum amount of ac power that the device can produce by inverting dc power. The rectifier capacity, which is the maximum amount of dc power that the device can produce by rectifying ac power, as a percentage of the inverter capacity has been specified [48].

Auxiliary power supply system includes auxiliary inverter and batteries. Auxiliary inverter supplies AC380V and DC24V to vehicles and charges the batteries. When high input voltage of DC 750V is not available (auxiliary inverter not working) for vehicles, it also supplies vehicles with control power and emergency power supply [44]. The model that suits this specification is a CyboEnergy Grid Interactive CI mini 1000A. It has 4 DC input channels and can produce 1150W, 380V 50HZ AC Power. Its lifetime is 10 years and its capital and replacement cost is USD600.

4.7 System schematic

After selecting all the above components, HOMER generates a schematic of the entire system as shown in figure 4-4.

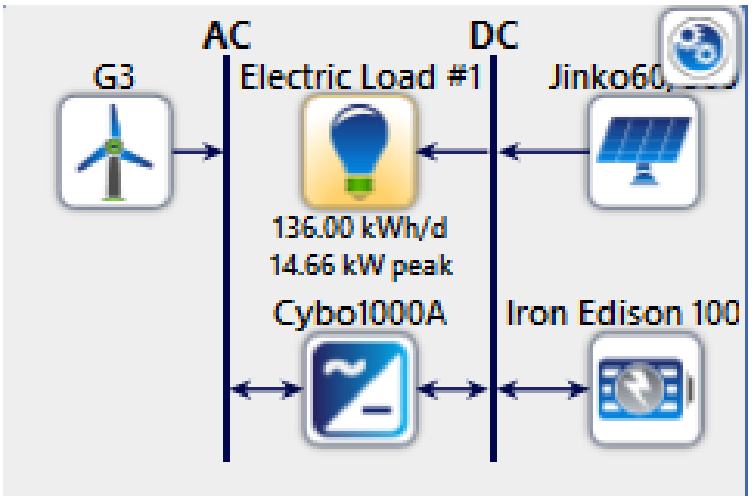

Figure 4-4: System schematic

From the schematic, the following can be adduced;

- Jinko60, is the solar system, which supplies direct current to the DC bus

- Iron Edison 100, is the battery for storing the excess energy generated
- G3 is the wind turbine that produces alternating current to the AC bus
- Cybo1000A is the converter which converts AC to DC to supply the electrical load

4.8 Simulation Results

The software gives a variety of options, over 1000 different options which are ranked in ascending order of the Cost of Energy and Net Present Cost. The list of possible combinations was truncated and the results obtained are presented in table 4-1.

Table 4-1: Simulation results

Solar PV(kW)	Wind turbine/G3	Battery(Ah)	Converter(kW)	Dispatch	COE ($)	NPC ($)	Operating cost ($/yr)	Initial capital ($)	Solar PV Capital Cost ($)	Solar PV/Production (kWh/yr)	Wind/Production (kWh/yr)
32.8	1	169	1.15	CC	0.0836	35872	188.6	39726	22643.4	59804	11577
31.6		176		CC	0.0947	42165	236.0	38923	21851	57711.6	
177.6				CC	0.3149	123078	34.83	122628	122628	323878	
177.6	1		1.15	CC	0.3305	129142	449.3	123333	122643	323919	11577

The most optimal combination is option 1 in table 4-1 and the electricity contribution for each of the power sources is shown in figure 4-5 below.

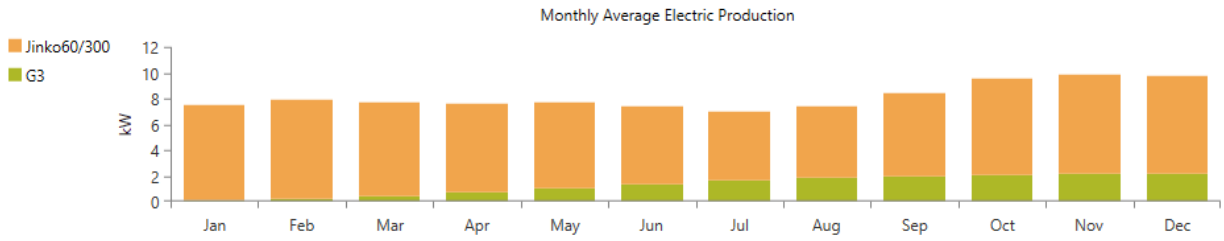

Figure 4-5: Monthly Average Electric Production for the optimal combination

4.8.1 Discussion

From the results obtained in table 4-1, the best optimal combination is Solar PV, wind and battery with a Cyclic Charge dispatch strategy, this means the system operates at full output power to serve the primary load, and any surplus electrical production goes towards the lower priority objectives. The CoE which is the average cost per kWh of useful

electrical energy produced by the system is 0.0836 and the Net Present Cost (NPC) is $ 35872.The Net Present Cost is the present value of all costs that the system incurs over its lifetime minus the present value of all the revenue it earns over its lifetime..

From Figure 4-5, it can be observed that the solar PV contributes the biggest amount of electricity throughout the year. The wind turbine only produces power from March to December. This is mainly because of the assumed wind speeds in these months, other months have lower wind speeds which are below the cut-in wind speed of the turbine and therefore no electric production takes place during this time.

In reality, this means that the turbine shall produce maximum energy when the train moves at maximum speed of 30km/h however at lower speeds, a reasonable amount of energy can be produced.

4.9 Sensitivity Analysis

The factors affecting electric production are wind speeds and solar irradiation and therefore these were used to do a sensitivity analysis. The sensitivity analysis is carried out to predict what would happen if operating conditions changed. Different values of solar irradiation were fed into the system, these included 2, 3, 4, 5, 6, 7, kW/h/m^2/day. Also, different wind speeds were fed into the system, these were 2, 4, 6, 12 and 15m/s. HOMER combines these different parameters and optimizes for the best possible combination. The results obtained were sorted for the lowest possible and COE and NPC and are presented in table 4-2.

Table 4-2: Sensitivity Analysis Results

Solar Irradiation (kWh/mÂ²/day)	Wind Speed (m/s)	Solar PV (kW)	Wind Power/G3	Battery	Converter (kW)	Dispatch	COE ($)	NPC ($)
5.8	12	31.6591		176		CC	0.08377	35872.0
5.8	15	31.6591		176		CC	0.08377	35872.0
5.8	2	31.6591		176		CC	0.08377	35872.0
5.8	4	31.6591		176		CC	0.08377	35872.0
5.8	6	31.6591		176		CC	0.08377	35872.0
5.8	9.5	31.6591		176		CC	0.08377	35872.0
6	12	29.6924		185		CC	0.08194	35217.8
6	15	29.6924		185		CC	0.08194	35217.8

Solar Irradiation (kWh/mÂ²/day)	Wind Speed (m/s)	Solar PV (kW)	Wind Power/G3	Battery	Converter (kW)	Dispatch	COE ($)	NPC ($)
6	2	29.6924		185		CC	0.08194	35217.8
6	4	29.6924		185		CC	0.08194	35217.8
6	6	29.6924		185		CC	0.08194	35217.8
6	9.5	29.6924		185		CC	0.08194	35217.8
7	12	29.9800		154		CC	0.07739	32977.6
7	15	29.9800		154		CC	0.07739	32977.6
7	2	29.9800		154		CC	0.07739	32977.6
7	4	29.9800		154		CC	0.07739	32977.6
7	6	29.9800		154		CC	0.07739	32977.6
7	9.5	29.9800		154		CC	0.07739	32977.6

4.9.1 Discussion of results

From table 4-2, it's observed that the lowest CoE, 0.073954 is obtained at higher values of solar irradiation i.e. 7kWh/m^2/day and higher wind speeds. It should be also noted that this cost of energy is lower than what was obtained in table 4-1, where the average solar irradiation is 5.8kWh/m^2/day. This implies that the higher the solar radiation and wind speeds, the lower the cost of energy since both systems would produce more energy at the same cost. However, in all instances, it shows no wind energy shall be produced. At this point, it's more cost effective to run the solar system alone as is shown in the table, in other words the solar system is able to supply sufficient power required for the entire system.

4.10 Adding Hydro power to the system

To compare the PV- wind hybrid system against the existing the hydroelectric power, a grid connection is added into the system. The initial capital to install the system is taken to be 0 since the system is already installed at AALRT and the cost of the unit of power for industrial purposes is taken to be $ 0.03 [60]. Once the system is connected to the grid, the schematic becomes as in figure 4-6 below.

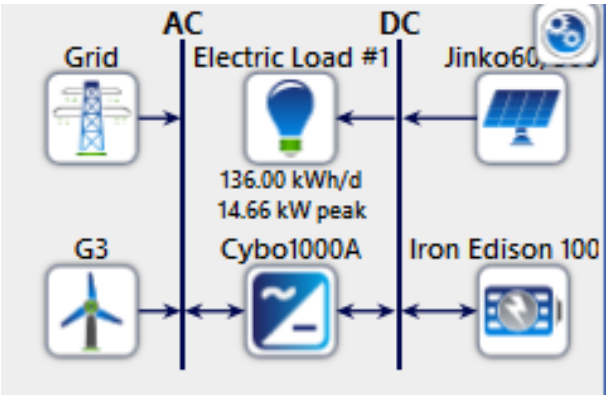

Figure 4-6: Schematic of the system when connected to the grid

At the prevailing conditions, the optimization results obtained are shown in table 4-3 below.

Table 4-3: Simulation Results with Grid connection

Solar PV (kW)	Wind/G3	Battery	Grid (kW)	Converter(kW)	Dispatch	COE ($)	NPC ($)
167.9722		10	999999	1.15	CC	0.251604	115048.1
177.6719			999999	1.15	CC	0.267056	121150.3
169.1094	1	9	999999	1.15	CC	0.276169	131125.5
177.6719	1		999999	1.15	CC		136498.2

It can be observed that the CoE for the optimal combination has increased to $ 0.251 as compared to the previous solar wind hybrid which is $0.083.

The average monthly power production for the most optimal combination shown above is graphically represented in figure 4-7 below. As can be observed, solar power supplies most of the power needed by the systems.

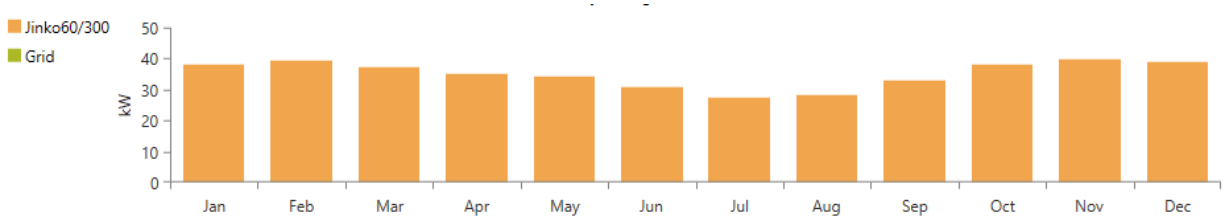

Figure 4-7: Average monthly electric power production

4.10.1 Sensitivity Analysis

While connected to the grid, the ever increasing price of a unit of power is always the biggest challenge. Therefore, to do a sensitivity analysis the cost of electricity is considered. It's assumed the price can go as high up as $1.00(worst case scenario) and the results obtained are presented in table 4-4.

Table 4-4: Sensitivity Analysis Results with grid connection

Power Price ($/kWh)	Solar PV(kW)	Wind Turbine/G3	Battery	Grid (kW)	Converter (kW)	Dispatch	COE ($)	NPC ($)
0.03	167.9722		10	999999	1.15	CC	0.251604	115048.1
0.5	167.9722		10	999999	1.15	CC	0.251604	115048.1
1	167.9722		10	999999	1.15	CC	0.251604	115048.1

4.10.2 Discussion of Results

As can be observed in table 4-4, the cost of energy remains almost the same at different prices of power. This literally means that the increase in price of power up to $1.00 has no significant impact on the net present cost and the cost of producing energy. This could be explained by the fact that the cost of energy is much lower at in all instances thus neutralizing the resulting effect from the increament of the unit cost of hydro power.

It's thus observed that in all instances, solar energy is the best optimal method of generating power at the train rooftop. Other factors that favor solar over wind energy are listed below;

- Installing solar panels is simple i.e. as soon as the panels are fixed then generation of power starts there and then. Depending on their angle and placement, you'll start storing solar energy right away. Wind power requires tall turbines to turn the wind

into electricity. The process can be complicated depending on turbine size and location.

- The effect of train performance on train performance is only as a result of the additional weight however a wind turbine increases both the weight and drag of the train therefore affecting performance more drastically.
- Turbines both large and small are noisy. Solar power, however, is silent, this is less irritating to passengers and the people in the neighborhood. This partly improves ride comfort.
- Solar panel maintenance is minimal because the panels are either stationary or close to it, depending on the system. Wind energy, however, features moving parts that can malfunction or break, and require fixing before they're up and running again.
- Solar systems can easily follow the sun as it moves throughout the day with the help of tracking systems. You can produce solar power even on cloudy days, whereas wind turbines will not run without the wind.

CHAPTER 5 CONCLUSIONS AND RECCOMENDATIONS

5.1 CONCLUSIONS

This thesis was done firstly to assess the wind and solar energy potential of Addis Ababa and more specifically on the train rooftop at AALRT. The amount of solar radiation that strikes the roof of the train on average ranges between 6.3 kWh/m^2/day to 7.6 kWh/m^2/day, this is sufficient to produce enough solar energy for the auxiliary power supply system.

The auxiliary power system for the units at AALRT is 8kW/12V, and the available rooftop area to install solar panels is 62.2m^2, allowing spacing between panels of 0.25m, allows only 21 panels to be installed. This has potential of generating 24.6kW/day if each panel is rated 300W.The excess energy can then be used for other purposes like motive power and can be supplied to the grid.

The ambient wind speeds in Addis Ababa are rather low and are not sufficient to produce wind energy however when the train is in motion, it induces higher than ambient wind speeds. Train speeds at AALRT range between 0m/s and 8.3m/s which are rather low. The cut in wind speed for most wind turbines is 3m/s and can go to as high up as 15m/s. And because most train stations are close to each other i.e. 1.3km [44], the train driver doesn't normally accelerate to the maximum speed which is 30km/hr or 8.3m/s. This means the average train speed in different sections is lower. This further limits the amount of wind energy that can be generated. This therefore is the reason why the turbine should be placed in a conical duct to improve these wind speeds. This further explains why in all the simulations, wind energy was the lowest contributor to the total energy required.

From the simulations, it was realized that the optimal method of generating energy for the auxiliary systems is by using solar. In most of the results obtained, solar was the sole supplier of the most of the power needed for the systems. This could be partly because of the large surface area available on the rooftop which means more solar panels can be installed and also the good solar potential of Addis Ababa plus the low maintenance cost of the solar system.

5.2 RECOMMENDATIONS

To improve wind speeds on the vehicle rooftop so as to generate more wind energy, the wind turbine should be placed in a duct. A duct is a tube, canal which can be used to convey a fluid or gas. In this case, it's designed in such a way that it can reduce the drag force and increase the velocity of air hitting the turbine blades. The duct and turbine are designed symmetrically in such a way that the turbine blades rotate irrespective of the wind direction. The entry portion of the duct is designed like a converging nozzle so that the velocity of the air is increased as it reaches the turbine blades. The exit portion is designed as a diverging nozzle so that the air expands and gets cooled as it exits the turbine without causing any resistance to train performance.

To overcome the effect of motion on the solar panels, a solar tracking system should be used so that position of the solar panels is able to change timely with the direction of the radiation. This would increase the efficiency of the whole system. While installing these systems, care should be taken not interrupt the other systems that are already running.

This wind energy generation project is more suitable for the Ethio-Djibout line as opposed to AALRT since it's a longer route and the trains move at a relatively higher speeds i.e. 120km/hr with minimal stopovers.

REFERENCES

[1] "UNDP," 14 11 2018. [Online]. Available: 1) http://hdr.undp.org/en/countries/profiles/ETH. [Accessed 14 11 2018].

[2] S. Fitwi, Feasibility Study of Standalone PV/Wind/Biogas Hybrid System for, Addis Ababa, 2014.

[3] 2. S. (. Ltd, "Africa's Power Journal," 2018 Spintelligent (PTY) Ltd, 1996. [Online]. Available: https://www.esi-africa.com/top-stories/153mw-adama-wind-farm-grows-ethiopias-renewable-energy-plan/. [Accessed 28 June 2019].

[4] G. t. E. r. G. (. hilawe Lakew, "Low Carbon Africa- Ethiopia," Christian Aid, Addis Ababa, 2011.

[5] G. T. E. R. Hilawe Lakewu, "Solar Energy Vision For Ethiopia," Freiburg, Germany, Ethiopia, Addis Ababa, 2012.

[6] D. F. a. Mulugetta, "Assessment of solar and wind energy in Ethiopia. I. Solar," Addis Ababa, 1996.

[7] Wikipedia, "Wikipedia," Wikipedia, 30 June 2018. [Online]. Available: https://en.wikipedia.org/wiki/Renewable_energy_in_Ethiopia. [Accessed 28 06 2019].

[8] S. D. Gupta, "Design of wind and solar powered railway coaching stock". US Patent 899/KOL/2015, 11 9 2015.

[9] M. K. A. K. Imran Syed Huain Jaffery, "A study on the feasibility of solar powered railway system for light weight urban transport system," 2012.

[10] A. S. J. Nanditha R Gajanur, "Solar Powered Railway Track Monitoring System," 2016.

[11] "Indian Railways launches first solar-powered train," 14 July 2017. [Online]. Available: https://economictimes.indiatimes.com/industry/transportation/railways/indian-railways-launches-first-solar-powered-train/amount-of-power-generated/slideshow/59593927.cms. [Accessed 15 Nov 2018].

[12] G. T. AYELE, "Feasibility Study of Small Hydro/PV/Wind Hybrid for Rural electrification in Ethiopia," Addis Ababa, 2011.

[13] P. M. R, Wind and Solar Power Systems: Design, Analysis, and Operation. 2nd Ed, Boca Raton: Taylor & Francis Group, 2006.

[14] A. a. H. Luque, Handbook of Photovoltaic Science and Engineering, West Sussex, England: John Wiley & Sons Ltd., 2003.

[15] B. L. Diffey, What is light?Photodermatology, photoimmunology&photomedicine18(2), 68-74, 2002.

[16] M. M. D. Ross, "Snow and ice accumulation on photovoltaic arrays: An assessment of the TN conseil melting processing technology," Natural Resources Canada, , arennearenne, 1995.

[17] M. Z. &. D. M. A. Jacobson, "Providing all global energy with wind, water and solar power, Part I Technologies, energy resources, quantities and areas of infrastructure," 2011.

[18] R. &. Messenger, "Photovoltaic systems engineering.CRC press," 2010.

[19] M. A. &. Z. Z. Eltawil, "Grid-connected photovoltaic power systems: Technical and Potential Problems, A review, Renewable and sustainable energy reviews," 2010.

[20] L. D. R. A. L. S. &. I. A. P. Gao, "Parallel-connected solar PV system to address partial and rapidly fluctuating shadow conditions. Industrial Electronic," 2009.

[21] G. Boneya, "Design of a Photovoltaic - wind Hybrid Power Generation system for Ethiopian Remote Area," Addis Ababa, 2011.

[22] B. W. Duffie J.A., Solar Engineering of Thermal Processes, New York, 1991.

[23] S. Kiros, "ASSESSMENT OF RESOURCE POTENTIAL AND MODELING OF STANDALONE PV/WIND HYBRID SYSTEM FOR ELECTRIFICATION OF AXUM DISTRICT," Addis Ababa, 2014.

[24] Y. M. Francis Drake, "Assessment of Solar And Wind Energy Resources in Ethiopia," *Solar Energy,* vol. 57, no. 3, pp. 2015 -217, 1996.

[25] P. e. a. Breeze, Renewable Energy Focus Handbook, Oxford,UK: Elsevier Inc., 2009.

[26] H. D. B. a. R. J. M. Fernando D. B., Wind Turbine Control Systems, Principles, Modelling and Gain Scheduling Design, London: Springer-Verlag, 2007.

[27] G. Boyle, Renewable Energy – Power for a sustainable future, 1996.

[28] A. V, Fundamentals of Renewable Energy, Elsevier Inc., , 2005.

[29] Sindhuja.B, "A Proposal for Implementation of Wind Energy Harvesting in Trains," *International Conference on Control, Instrumentation, Energy & Communication*, pp. 696 - 702, 2014.

[30] M. B. A. S. H. B. Venera Nurmanova, "Feasibility Study on Wind Energy Harvesting System in Moving Trains," in *International Siberian Conference on Control and Communications*, Iran, 2017.

[31] A. V, Fundamentals of Renewable Energy processes, Elevesier Inc 2015, 2015.

[32] A. S. G. Garvit Josh, "Utilization of wind energy from Railways using Vertical axis wind turbine," *Research Gate*, vol. 1, no. ISSN: 10.1109, pp. 1-6, 2015.

[33] H. Nasser, "Vehicle Dynamics Conversion into Power (Dynapower)," *Scince Direct*, no. AASRI Procedia 7 (2014) 32 – 37, 2013.

[34] L. N. Srinivsan, "Design and Simulation of wind turbine on Rail coach for power Generation," *International Journal of Engineering Research and Technology*, vol. 6 , no. 2, pp. 635-638, 2017.

[35] P. B. K. Avinash Kumar, "Generating and Saving Wind energy by installing Wind turbines along railway tracks," *Research gate*, 2015.

[36] S. A. A. Salameh, "Rail Mounted Wind Turbine". USA Patent USOO9046O76B1, 2 June 2015.

[37] D. D. Dearborn, "MODULAR SOLAR PHOTOVOLTAIC CANOPY SYSTEM FOR DEVELOPMENT OR RAIL VEHICLE TRACTION POWRE". USA Patent US 2010O2O0041A1, 12 August 2010.

[38] G. V. J. S. S. K. R. M. Shravanth Vasisht, "Rail coaches with rooftop solar photovoltaic systems: A feasibility Study," *Science Direct*, 2016.

[39] G. P. a. T. Sudheshnan, "A RENEWABLE ENERGY APPROACH BY FAST MOVING VEHICLES," in *Proceedings of the National Seminar & Exhibition on Non-Destructive Evaluation*, 2011.

[40] N. R. Sofian Mohd, "An Evaluation of drag Coefficient of wind turbine system installed on moving car," *Applied Mechanics and Materials*, 2014.

[41] U. L. D. U. H. Hinrich Helms, "Energy savings by Light weighting, Final Report," Udo Lambrecht; IFEU-Institute Heidelberg, 2003.

[42] B. B. e. al, "Optimization of Hybrid Renewable Energy Power Systems- A Review," *NTERNATIONAL JOURNAL OF PRECISION ENGINEERING AND MANUFACTURING-GREEN TECHNOLOGY* , vol. 2, no. 1, pp. 99-112, 2015.

[43] H. Energy, "www.homerenergy.com," HOMER ENERGY, 2 December 2018. [Online]. Available: https://homerenergy.com/products/pro/index.html. [Accessed 2 Decemember 2018].

[44] C. R. G. Ltd, "Technical Specifications of Vehicles," 2013.

[45] NASA, "Surface Meteorology and Solar Energy/NASA Open Data Portal," NASA, [Online]. Available: https://data.nasa.gov/widgets/wn3p-qsan. [Accessed 28 01 2019].

[46] S. Kebele, "Design of a Hybrid Solar System for Locomotive use on the Ethio-Djiboute route," Addis Ababa, 2016.

[47] B. Supllies, "Solar Catalogue," Battery Supplies, France.

[48] T. Jima, "Simulation and Optimization of Wind Turbine, Solar PV, Storage Battery and Diesel Generator Hybrid Power System for a," Addis Ababa, 2013.

[49] R. M.R, "Small Wind / Photovoltaic Hybrid Renewable Energy System Optimisation, Msc Thesis," University of Puerto, 2008.

[50] 2. Sunmetrix, "SUNMetrix," sunmetrix, 2012. [Online]. Available: https://sunmetrix.com/is-my-roof-suitable-for-solar-panel-and-what-is-the-weight-of-the-solar-panel/. [Accessed 17 02 2019].

[51] S. V. Abraham, "Power Generation from a Moving Locomotive by WInd Turbine," *Global Research and Development Journal for Engineering,* no. e-ISSN 2455-5703, p. March, 2018.

[52] S. V. Abraham, "Power Generation from a Moving Locomotive by Wind Turbine," *Global Research and Development Journal for Engineering,* vol. 04, no. 02, pp. 2455-5703, 2018.

[53] D. G. B. R. Sagar Ingle, "Wind Power Generation System Using Railway – A Prototype Mode," *International Journal of Emerging Trends in Science and Technology,* vol. 02, no. 03, pp. 1991-1994, 2015.

[54] Wikipedia, "Drag Coefficient," WIkipedia, 29 06 2019. [Online]. Available: https://en.wikipedia.org/wiki/Drag_coefficient. [Accessed 3 July 2019].

[55] B. Ali, "Hybrid Photovoltaic Diesel System in a Cable Car Resort Facility," *European Journal of Scientific Research,* vol. 26, no. 1, 2010.

[56] G. B. Huka, "DESIGN OF A PHOTOVOLTAIC-WIND HYBRID POWER GENERATION SYSTEMFOR ETHIOPIAN REMOTE AREA," Addis Ababa, 2011.

[57] B. Getachew, "Study into the Potential and Feasibility of a Standalone Solar-wind Hybrid Electric Supply system for Ethiopia," Royal Institute of Technology, KTH, 2009.

[58] "HOMER, the micropower optimization model," HOMER, 2008. [Online]. Available: http://www.nrel.gov/homer. [Accessed 3 March 2019].

[59] N. K. R. Md. Nurunnabi, "Grid Connected Hybrid Power System Design Using Homer," *International Conference on Advances in Electrical Engineering,* 2015.

[60] C. t. travel, "Cost to travel," Cost to travel, 2015. [Online]. Available: https://www.costtotravel.com/cost/electricity-in-ethiopia. [Accessed 05 05 2019].

APPENDICES

APPENDIX A: Total Sunshine Hours for Addis Ababa for 2016 and 2017

Name	Elevation	Geogr1	Geogr2	element	Year	Month	1	2	3	4	5	6	7	8	9	10	11	12	13	14	15	16	17	18	19	20	21	22	23	24	25	26	27	28	29	30	31
Addis Ababa Obs	2386	38.7475	9.01891	SUNHRS	2016	01	8.0	10.2	10.3	5.6	10.0	8.3	10.0	9.0	7.2	8.5	8.8	3.0	2.2	4.7	4.2	4.4	3.5	6.5	7.0	8.7	7.6	10.0	10.2	8.2	10.2	10.3	8.6	6.7	3.4	6.4	6.5
Addis Ababa Obs	2386	38.7475	9.01891	SUNHRS	2016	02	9.2	10.3	8.6	10.4	8.7	10.3	9.5	7.8	9.8	9.5	9.3	9.8	9.7	9.8	10.2	10.0	7.8	8.9	10.2	9.0	10.0	9.2	9.3	8.0	4.5	6.1	8.0	10.0	10.0		
Addis Ababa Obs	2386	38.7475	9.01891	SUNHRS	2016	03	8.8	9.2	7.6	7.4	8.3	6.5	6.4	5.2	6.3	4.9	10.3	10.3	10.3	10.4	10.6	10.7	9.7	8.5	9.0	8.0	8.3	4.8	5.5	3.4	6.0	5.5	4.7	7.0	6.2	7.9	8.6
Addis Ababa Obs	2386	38.7475	9.01891	SUNHRS	2016	05	4.2	3.0	6.6	8.2	8.9	4.2	2.5	5.4	4.4	0.4	0.2	5.6	6.6	9.8	10.3	8.3	2.4	3.5	5.6	8.0	9.7	5.6	4.2	3.2	3.3	2.6	6.1	6.8	9.3	7.8	10.0
Addis Ababa Obs	2386	38.7475	9.01891	SUNHRS	2016	06	7.6	6.5	6.0	7.8	3.0	5.6	4.0	4.5	5.6	5.2	3.9	10.2	7.5	1.2	5.0	6.0	2.6	0.3	1.1	0.3	3.6	3.8	6.7	2.0	3.0	3.0	2.2	1.2	0.9	3.8	
Addis Ababa Obs	2386	38.7475	9.01891	SUNHRS	2016	08	2.5	1.6	0.1	0.4	0.0	1.0	2.0	0.6	0.1	0.1	2.7		5.2	5.4	3.0	6.5	2.3	1.5	0.0	0.1	1.9	5.7	4.5	5.5	1.6	6.5	5.3	4.0	1.8	2.2	3.9
Addis Ababa Obs	2386	38.7475	9.01891	SUNHRS	2016	09	0.7	0.0	2.5	9.4	10.1	9.5	7.5	0.0	3.2	5.2	5.1	3.3	3.6	3.5	9.8	7.2	2.2	1.7	2.3	3.1	4.5	10.0	5.2	2.5	1.8	3.7	1.8	5.2	5.1	1.2	
Addis Ababa Obs	2386	38.7475	9.01891	SUNHRS	2016	10	3.4	1.6	9.4	9.7	4.7	8.6	8.7	10.4	10.1	6.4	3.3	2.3	5.7	6.3	6.2	8.8	10.2	9.2	10.3	8.5	5.5	2.0	6.2	7.8	8.2	10.2	10.5	10.3	8.2	10.5	10.5
Addis Ababa Obs	2386	38.7475	9.01891	SUNHRS	2016	11	10.9	9.8	10.3	10.2	10.2	10.2	9.7	0.6	1.3	10.2	8.4	1.3	8.4	10.3	10.4	10.2	8.3	10.0	9.9	10.2	7.8	10.1	7.5	5.6	7.0	3.5	2.0	1.4	10.2	8.8	
Addis Ababa Obs	2386	38.7475	9.01891	SUNHRS	2016	12	5.8	2.3	10.3	10.5	8.6	10.4	10.0	9.5	10.4	10.4	10.3	9.2	10.2	8.6	9.4	10.0	8.7	10.4	10.3	8.4	8.7	8.6	10.2	10.4	8.5	10.4	10.3	9.0	10.0	10.1	10.3
Addis Ababa Obs	2386	38.7475	9.01891	SUNHRS	2017	01	10.2	10.5	10.3	9.3	9.2	10.4	10.4	10.5	10.4	10.4	8.2	10.5	10.4	9.9	10.3	10.0	10.3	10.2	10.4	10.2	10.0	9.5	10.3	9.7	10.0	10.2	10.3	10.0	7.8	10.0	10.0
Addis Ababa Obs	2386	38.7475	9.01891	SUNHRS	2017	02	10.0	10.0	10.3	6.6	10.4	8.2	10.2	9.6	10.1	9.8	5.2	5.5	3.1	1.6	9.8	10.4	9.6	8.8	5.3	10.3	10.4	10.3	10.0	8.0	3.5	6.3	2.0	6.0			
Addis Ababa Obs	2386	38.7475	9.01891	SUNHRS	2017	03	10.2	10.3	10.0	10.0	10.3	9.7	10.3	9.2	10.2	10.0	10.6	9.8	8.3	10.7	9.0	10.0	10.1	9.2	7.8	7.0	6.7	7.8	4.2	5.2	5.0	2.7	7.0	5.3	3.0	8.8	6.5
Addis Ababa Obs	2386	38.7475	9.01891	SUNHRS	2017	04	9.3	8.3	10.6	8.5	9.8	10.6	6.5	9.6	10.5	10.6	10.8	10.6	8.7	10.3	9.8	7.8	10.1	8.2	10.2	7.0	8.5	6.0	10.7	9.8	7.6	8.7	7.4	3.1	0.0	2.0	
Addis Ababa Obs	2386	38.7475	9.01891	SUNHRS	2017	06	6.5	9.0	8.0	5.2	6.1	6.5	7.0	4.1	7.0	0.0	4.2	2.7	5.1	5.4	10.0	6.6	5.5	4.0	3.5	8.2	8.4	6.5	6.3	5.0	1.2	3.9	0.8	2.1	6.5	5.2	
Addis Ababa Obs	2386	38.7475	9.01891	SUNHRS	2017	07	0.4	4.5	0.0	1.3	3.2	3.4	2.2	0.8	0.1	5.2	1.5	4.2	1.5	2.3	3.5	3.7	2.8	4.1	1.2	1.2	2.2	1.9	1.6	4.3	2.0	0.7	3.5	2.5	5.0	2.5	1.5
Addis Ababa Obs	2386	38.7475	9.01891	SUNHRS	2017	08	2.0	3.4	4.2	4.5	1.2	3.6	0.7	0.0	2.0	3.0	1.2	2.0	0.6	2.3	4.8	5.7	5.8	2.5	5.5	5.0	5.5	3.3	2.2	1.4	2.9	0.6	1.8	3.0	0.0	1.5	3.2
Addis Ababa Obs	2386	38.7475	9.01891	SUNHRS	2017	09	1.9	3.5	1.4	2.5	2.6	2.5	2.4	5.5	5.1	3.3	4.8	9.7	10.4	3.9	4.0	1.5	1.8	1.8	2.4	2.8	3.5	1.4	4.2	5.2	1.3	5.9	8.2	6.5	0.6	0.0	
Addis Ababa Obs	2386	38.7475	9.01891	SUNHRS	2017	11	9.8	8.2	10.0	6.8	3.7	5.2	5.0	8.3	10.0	9.8	9.0		7.5	10.2	10.4	10.4	10.0	8.5	10.0	10.3	10.2	10.0	10.0	9.8	7.4	9.5	10.4	10.0	6.4	10.1	
Addis Ababa Obs	2386	38.7475	9.01891	SUNHRS	2017	12	10.5	9.0	10.0	10.4	8.0	9.8	8.5	9.3	9.6	10.0	10.3	9.4	9.6	9.7	9.9	10.0	9.3	9.5	10.1	10.2	10.6	9.8	9.9	10.3	9.2	10.2	9.0	9.9	10.4	10.1	9.9

APPENDIX B: Wind Speed Measured at Addis Ababa

Name	Elevation	Geogr1	Geogr2	element	Year	Jan	Feb	Mar	Apr	May	Jun	Jul	Aug	Sep	Oct	Nov	Dec
Addis Aba	2386	38.7475	9.01891	WINDLY	2016	0.8	0.9	0.9	0.6	0.6	0.5	0.5	0.4	0.5	0.6	0.7	0.7
Addis Aba	2386	38.7475	9.01891	WINDLY	2017	0.6	0.7			0.6			0.3	0.4		0.6	

APPENDIX C: Solar Radiation Estimation Using the Mathematical approach

Solar Radiation for 2016

The values of constant a and b are 0.191 and 0.622 respectively as obtained by Drake and Mulugeta, 1996

Month	n	Ø	∂	w_s	N	(360*N/365)	Cos(360*N/365)	Cos(Ø)	$Cos(\partial)$	(3.14*w)/180)	Sin(w)	Sin(Ø)	$Sin(\partial)$	H_0 (MJ/m^2)	H (MJ/m^2)	(H * 277.78) kWh/m2
Jan	7.4	9.02	-20.9	84.5	11.2	11	0.981	0.987	0.934	1.474	0.995	0.1567	-0.357	32.5	19.5	**5.4**
Feb	9.1	9.02	-13	86.7	11.6	11.4	0.98	0.987	0.974	1.512	0.998	0.1567	-0.225	35.2	23.9	**6.6**
Mar	7.6	9.02	-2.4	89.4	11.9	11.7	0.979	0.987	0.999	1.560	1.000	0.1567	-0.042	37.9	22.3	**6.2**
Apr		9.02	9.4	92.4	12.3	12.1	0.978	0.987	0.987	1.612	0.999	0.1567	0.163	39.4	7.5	**2.1**
May	5.7	9.02	18.8	94.9	12.7	12.5	0.976	0.987	0.947	1.655	0.996	0.1567	0.322	39.4	18.5	**5.1**
June	4.1	9.02	23.1	96.1	12.8	12.6	0.976	0.987	0.920	1.676	0.994	0.1567	0.392	39.1	15.3	**4.2**
July		9.02	21.2	95.5	12.7	12.5	0.976	0.987	0.932	1.666	0.995	0.1567	0.361	39.3	7.5	**2.1**
Aug	2.6	9.02	13.15	93.3	12.4	12.2	0.977	0.987	0.974	1.628	0.998	0.1567	0.227	39.5	12.7	**3.5**
Sept	4.4	9.02	2.2	90.5	12.1	11.9	0.978	0.987	0.999	1.579	1.000	0.1567	0.038	38.7	16.1	**4.5**
Oct	7.5	9.02	-9.6	87.5	11.7	11.5	0.979	0.987	0.986	1.526	0.999	0.1567	-0.167	36.2	21.4	**5.9**
Nov	7.8	9.02	-18.1	85.3	11.4	11.2	0.981	0.987	0.951	1.488	0.997	0.1567	-0.311	33.5	20.7	**5.7**
Dec	9.4	9.02	-23	83.9	11.2	11	0.982	0.987	0.921	1.464	0.994	0.1567	-0.391	31.6	22.6	**6.3**

	Solar Radiation for 2017															
Month	**n**	**Ø**	**∂**	**w_s**	**N**	**(360*N/365)**	**Cos(360*N/365)**	**Cos(Ø)**	**$Cos(\partial)$**	**(3.14*w)/180)**	**Sin(w)**	**Sin(Ø)**	**$Sin(\partial)$**	**H_0 (MJ/m^2)**	**H (MJ/m^2)**	**(H * 277.78) kWh/m2**
Jan	10	9.02	-20.9	84.5	11.2	11	0.981	0.987	0.934	1.474	0.995	0.1567	-0.357	32.5	24.2	**6.7**
Feb	7.9	9.02	-13	86.7	11.6	11.4	0.98	0.987	0.974	1.512	0.998	0.1567	-0.225	35.2	21.7	**6.0**
Mar	8.2	9.02	-2.4	89.4	11.9	11.7	0.979	0.987	0.999	1.560	1.000	0.1567	-0.042	37.9	23.5	**6.5**
Apr	8.4	9.02	9.4	92.4	12.3	12.1	0.978	0.987	0.987	1.612	0.999	0.1567	0.163	39.4	24.3	**6.7**
May		9.02	18.8	94.9	12.7	12.5	0.976	0.987	0.947	1.655	0.996	0.1567	0.322	39.4	7.5	**2.1**
June	5.4	9.02	23.1	96.1	12.8	12.6	0.976	0.987	0.920	1.676	0.994	0.1567	0.392	39.1	17.7	**4.9**
July	2.4	9.02	21.2	95.5	12.7	12.5	0.976	0.987	0.932	1.666	0.995	0.1567	0.361	39.3	12.1	**3.4**
Aug	2.8	9.02	13.15	93.3	12.4	12.2	0.977	0.987	0.974	1.628	0.998	0.1567	0.227	39.5	13.1	**3.6**
Sept	3.7	9.02	2.2	90.5	12.1	11.9	0.978	0.987	0.999	1.579	1.000	0.1567	0.038	38.7	14.7	**4.1**
Oct		9.02	-9.6	87.5	11.7	11.5	0.979	0.987	0.986	1.526	0.999	0.1567	-0.167	36.2	6.9	**1.9**
Nov	8.9	9.02	-18.1	85.3	11.4	11.2	0.981	0.987	0.951	1.488	0.997	0.1567	-0.311	33.5	22.7	**6.3**
Dec	9.8	9.02	-23	83.9	11.2	11	0.982	0.987	0.921	1.464	0.994	0.1567	-0.391	31.6	23.3	**6.5**

	Solar Radiation for 2018															
Month	**n**	**Ø**	**∂**	**W_s**	**N**	**(360*N/365)**	**Cos(360*N/365)**	**Cos(Ø)**	**$Cos(\partial)$**	**(3.14*w)/180)**	**Sin(w)**	**Sin(Ø)**	**$Sin(\partial)$**	**H_0 (MJ/m^2)**	**H (MJ/m^2)**	**(H * 277.78) kWh/m2**
Jan	8.3	9.02	-20.9	84.5	11.2	11	0.981	0.987	0.934	1.474	0.995	0.1567	-0.357	32.5	21.2	**5.9**
Feb	8.6	9.02	-13	86.7	11.6	11.4	0.98	0.987	0.974	1.512	0.998	0.1567	-0.225	35.2	23.0	**6.4**
Mar	7.1	9.02	-2.4	89.4	11.9	11.7	0.979	0.987	0.999	1.560	1.000	0.1567	-0.042	37.9	21.3	**5.9**
Apr	7.8	9.02	9.4	92.4	12.3	12.1	0.978	0.987	0.987	1.612	0.999	0.1567	0.163	39.4	23.1	**6.4**
May	6.7	9.02	18.8	94.9	12.7	12.5	0.976	0.987	0.947	1.655	0.996	0.1567	0.322	39.4	20.5	**5.7**
June	5.5	9.02	23.1	96.1	12.8	12.6	0.976	0.987	0.920	1.676	0.994	0.1567	0.392	39.1	17.9	**5.0**
July	3.8	9.02	21.2	95.5	12.7	12.5	0.976	0.987	0.932	1.666	0.995	0.1567	0.361	39.3	14.8	**4.1**
Aug	2.9	9.02	13.15	93.3	12.4	12.2	0.977	0.987	0.974	1.628	0.998	0.1567	0.227	39.5	13.3	**3.7**
Sept		9.02	2.2	90.5	12.1	11.9	0.978	0.987	0.999	1.579	1.000	0.1567	0.038	38.7	7.4	**2.1**
Oct	6.7	9.02	-9.6	87.5	11.7	11.5	0.979	0.987	0.986	1.526	0.999	0.1567	-0.167	36.2	19.8	**5.5**
Nov	8.1	9.02	-18.1	85.3	11.4	11.2	0.981	0.987	0.951	1.488	0.997	0.1567	-0.311	33.5	21.2	**5.9**
Dec	9.5	9.02	-23	83.9	11.2	11	0.982	0.987	0.921	1.464	0.994	0.1567	-0.391	31.6	22.7	**6.3**

Annual Average

Month	Solar Radiation, kW/h/day			
	2016	2017	2018	Average
Jan	5.4	6.7	5.9	6.0
Feb	6.6	6.0	6.4	6.3
Mar	6.2	6.5	5.9	6.2
Apr	2.1	6.7	6.4	5.1
May	5.1	2.1	5.7	4.3
June	4.2	4.9	5.0	4.7
July	2.1	3.4	4.1	3.2
Aug	3.5	3.6	3.7	3.6
Sept	4.5	4.1	2.1	3.5
Oct	5.9	1.9	5.5	4.5
Nov	5.7	6.3	5.9	6.0
Dec	6.3	6.5	6.3	6.3